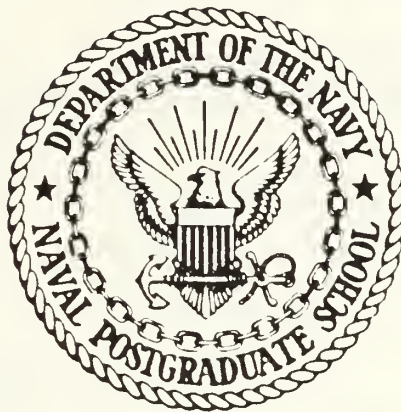# NAVAL POSTGRADUATE SCHOOL
Monterey, California

THESIS

THE RELATIONSHIP BETWEEN
MARINE AEROSOL OPTICAL DEPTH AND
SATELLITE-SENSED SEA SURFACE TEMPERATURE

by

Susan K. Runco

June 1986

Thesis Advisor: Philip A. Durkee

T232243

REPORT DOCUMENTATION PAGE

REPORT SECURITY CLASSIFICATION	1b. RESTRICTIVE MARKINGS
UNCLASSIFIED	

. SECURITY CLASSIFICATION AUTHORITY	3. DISTRIBUTION / AVAILABILITY OF REPORT
. DECLASSIFICATION / DOWNGRADING SCHEDULE	Approved for public release; distribution is unlimited.

PERFORMING ORGANIZATION REPORT NUMBER(S)	S. MONITORING ORGANIZATION REPORT NUMBER(S)
..	

NAME OF PERFORMING ORGANIZATION	6b OFFICE SYMBOL (If applicable)	7a. NAME OF MONITORING ORGANIZATION
Naval Postgraduate School	63	Naval Postgraduate School

ADDRESS (City, State, and ZIP Code)	7b. ADDRESS (City, State, and ZIP Code)
Monterey, California 93943-5000	Monterey, California 93943-5000

NAME OF FUNDING / SPONSORING ORGANIZATION	8b. OFFICE SYMBOL (If applicable)	9. PROCUREMENT INSTRUMENT IDENTIFICATION NUMBER

ADDRESS (City, State, and ZIP Code)	10 SOURCE OF FUNDING NUMBERS			
	PROGRAM ELEMENT NO.	PROJECT NO	TASK NO	WORK UNIT ACCESSION NO.

TITLE (Include Security Classification)
THE RELATIONSHIP BETWEEN MARINE AEROSOL OPTICAL DEPTH AND
SATELLITE-SENSED SEA SURFACE TEMPERATURE

PERSONAL AUTHOR(S)
Runco, Susan K.

TYPE OF REPORT	13b TIME COVERED	14 DATE OF REPORT (Year, Month, Day)	1S PAGE COUNT
Master's Thesis	FROM _____ TO _____	1986, June	77

SUPPLEMENTARY NOTATION

COSATI CODES			18 SUBJECT TERMS (Continue on reverse if necessary and identify by block number)
FIELD	GROUP	SUB-GROUP	Sea Surface Temperature, Optical Depth, Aerosol, Remote Sensing, Multichannel, Radiometer, Transmittance, Radiance, AVHRR, PRT-5, LOWTRAN

ABSTRACT (Continue on reverse if necessary and identify by block number)

Multichannel sea surface temperatures (MCSST) computed from NOAA-7 AVHRR channels 4 and 5 are compared to sea surface temperatures measured by an aircraft radiometer (PRT-5). This data set was collected in Fall, 1982 off the southern Californian coast. The MCSST was warmer by 0.82 degrees in the area where aerosol effects did not offset increasing radiance due to vertically warming air temperature. As aerosols were able to offset the temperature contribution to radiance, the difference between MCSST and PRT-5 SST measurements decreased.

Aerosol effects on infrared radiance were qualitatively examined using an atmospheric transmittance model (LOWTRAN 6). Comparing the model and PRT-5 results indicates that below the marine boundary layer, high aerosol extinction caused significant cooling. Above the boundary layer, aerosols scattered and emitted energy, generally decreasing the measured radiance. The emission moderated the decrease by increasing the radiance slightly.

DISTRIBUTION / AVAILABILITY OF ABSTRACT	21. ABSTRACT SECURITY CLASSIFICATION
☒ UNCLASSIFIED/UNLIMITED ☐ SAME AS RPT. ☐ DTIC USERS	UNCLASSIFIED

NAME OF RESPONSIBLE INDIVIDUAL	22b. TELEPHONE (Include Area Code)	22c. OFFICE SYMBOL
Philip A. Durkee	408-646-3465	63De

FORM 1473, 84 MAR   83 APR edition may be used until exhausted   SECURITY CLASSIFICATION OF THIS PAGE
All other editions are obsolete

The Relationship Between
Marine Aerosol Optical Depth and
Satellite-Sensed Sea Surface Temperature

by

Susan K. Runco
Lieutenant, United States Navy
B.S., Florida Institute of Technology, 1976

Submitted in partial fulfillment of the
requirements for the degree of

MASTER OF SCIENCE IN METEOROLOGY AND OCEANOGRAPHY

from the

NAVAL POSTGRADUATE SCHOOL
June 1986

ABSTRACT

Multichannel sea surface temperatures (MCSST) computed from NOAA-7 AVHRR channels 4 and 5 are compared to sea surface temperatures measured by an aircraft radiometer (PRT-5). This data set was collected in Fall, 1982 off the southern Californian coast. The MCSST was warmer by 0.82 degrees in the area where aerosol effects did not offset increasing radiance due to vertically warming air temperature. As aerosols were able to offset the temperature contribution to radiance, the difference between MCSST and PRT-5 SST measurements decreased.

Aerosol effects on infrared radiance were qualitatively examined using an atmospheric transmittance model (LOWTRAN 6). Comparing the model and PRT-5 results indicates that below the marine boundary layer, high aerosol extinction caused significant cooling. Above the boundary layer, aerosols scattered and emitted energy, generally decreasing the measured radiance. The emission moderated the decrease by increasing the radiance slightly.

TABLE OF CONTENTS

4

LIST OF FIGURES

5

LIST OF TABLES

ACKNOWLEDGEMENTS

I. <u>INTRODUCTION</u>

Infrared measurements from satellite mounted radiometers currently supply the quantity but not the degree of accuracy of sea surface temperature (SST) values required for work in many scientific fields, such as oceanography and meteorology. The accurate determination of SST from radiometer measurements requires improved methods for measuring and analyzing atmospheric data and a better understanding of the radiative transfer processes through the earth's atmosphere.

Improvements to satellite-derived SST have been made through multiple-wavelength techniques. Multispectral measurements from satellites facilitate calculation of atmospheric attenuation corrections to SST by combining brightness temperatures from two or three atmospheric windows. Each spectral band has a characteristic atmospheric transmittance which, when combined, can act as a weighting function to constants in multichannel sea surface temperature (MCSST) equations. Many MCSST procedures first do tests for initial cloud filtering using spectral measurements from the visible ranges (0.58 to 1.1 microns). Cloud tests for this study are not considered because the data analyzed came from cloud-free conditions. McClain (1980) develops MCSST equations by studying the relationships between model generated brightness temperatures in the infrared ranges of 3.7, 11 and 12 microns, to variations in atmospheric transmittance due to temperature and humidity. Further development of MCSST equations from Advanced Very High Resolution Radiometer (AVHRR) measurements are given in McClain et al. (1983). Strong and McClain (1984) adjust the temperature-dependant bias corrections of the MCSST equations on the basis of 164 match-ups with drifting buoy temperatures. They found root mean square differences of

0.68°C between satellite and buoys, whereas with ships-of-opportunity they were 1.8°C. This latest version of the MCSST equations is used for this study.

Both studies, by Strong and McClain (1984) and McClain et al. (1983), discuss briefly the problems associated with direct comparison of radiometer-measured "skin" SST and *in situ* "bulk" temperatures. The "skin" layer temperature is a result of a loss of energy from the sea surface to the atmosphere by molecular processes at the air-sea interface. As described in McAlister and McLeish (1969), this "skin" or thermal boundary layer ranges in depth of 0.1 to 1.0 millimeter within which the temperature increases linearly with depth. This temperature gradient is proportional to the net heat lost to the atmosphere and is in the range of 2 to 5°C per centimeter. The *in situ* bulk temperatures are collected from below this skin layer and are often several tenths of a degree different from the skin temperature.

This study is directed toward reducing the uncertainties in corrections for MCSST equations due to atmospheric effects. Specifically, aerosol effects on infrared radiance is investigated. Atmospheric effects are calculated from aircraft measurements of temperature, dewpoint, pressure and particle distribution. This is done using an atmospheric transmittance model called LOWTRAN 6, from the Air Force Geophysics Laboratory (Kneizys et al., 1984). The amount of component ,such as water vapor or aerosol, contributions to the total atmospheric effect is investigated by running the LOWTRAN 6 model with different input parameters.

Aerosol effects on infrared radiance are evident in both the MCSST from NOAA-7 satellite AVHRR channels 4 and 5 (11 and 12 μm respectively) and the aircraft radiometer (PRT-5, 8 through 14 μm) SST. The MCSST was compared with the PRT-5 SST measured at the lowest altitude of a vertical spiral. This comparison showed that the difference between the PRT-5

and satellite SST was larger in areas where cooling due to aerosol absorption and scattering did not offset the increasing effect that warming air temperature, with height, had on radiance measurements. The satellite SST was warmer by $0.82^{\circ}C$ in the area of highest tropospheric aerosol concentration. Yet, the resulting low transmittance could not offset the warm air temperature's effect on measured radiance. The size or quantity of aerosols did not make the transmittance low enough to offset the warming above the marine boundary layer. As the aerosols were able to offset the increase in air temperature, the variance between the SSTs decreased. Comparing the LOWTRAN model and PRT-5 results confirms that, for this period, air temperature, aerosols and water vapor density are the major influences on radiometer-measured SST.

With further quantitative research and analysis, these results coupled with methods to measure vertical profiles and aerosol characteristics, can be applied to current corrections for MCSST and used to develop other multichannel combinations to improve the accuracy of satellite sensed SST.

II. DATA AND PROCEDURES

A. DATA SOURCES

Data sources for this study are coincident measurements taken from the NOAA-7 AVHRR, an aircraft mounted radiometer (PRT-5), and other aircraft environmental data sensors. Flights were conducted during the period of 20 September through 7 October 1982 off the coast of southern California. Fig. 2.1 shows the area and specific locations of aircraft vertical spiral data used for analysis.
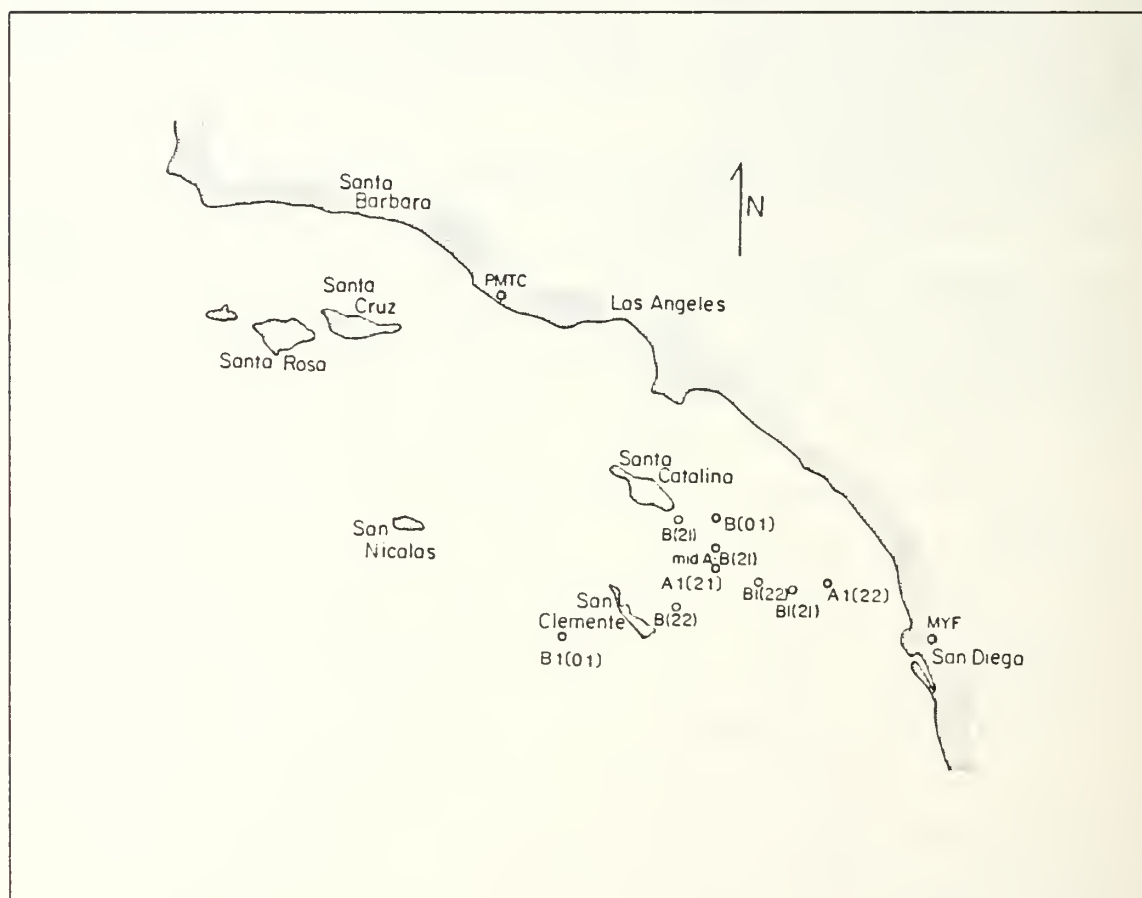

Figure 2.1   Locations of aircraft spirals.

12

Prior to flight, satellite images were used to locate regions of brightness variation which were expected to be caused by aerosol variation. Fett and Isaacs (1979) discussed the relationship between the variations of relative humidity and aerosols which are evident as 'anomalous gray-shades' or brightness variations. Griggs (1983) demonstrated the usefulness in using satellite sensors, such as the NOAA-7 AVHRR channels 1 and 2, to measure tropospheric aerosols and Durkee et al. (1984) summarized the ability of the meteorological satellites to detect marine aerosol particle variations. The aircraft was then directed to these regions by radio. The experimental instruments, measurement procedures and data reduction, and analyses are discussed in the following paragraphs to provide a basis for understanding the results and conclusions.

1. The NOAA-7 AVHRR

The NOAA-7 satellite is in sun-synchronous polar orbit. It crosses the equator at about 1430 (ascending; increasing north latitude) and 0230 (descending; decreasing north latitude) Local Solar Time. Since the orbit does not cross at the same position each day, the afternoon passage time over southern California varied from 1430 to 1600 Pacific Daylight Time (PDT).

The swath width of the AVHRR is approximately 2580 km. It collects data at 2048 discrete points across its path and has a surface resolution for each 'picture element' or 'pixel' of 1.1 km at the subsatellite point which expands to several kilometers at the edges of the coverage. The AVHRR measures radiance in 5 spectral bands. The wavelength bands, in microns, are as follows: Channel 1 (red-visible), 0.58-0.68; Channel 2 (near-infrared), 0.725-1.10; Channels 3, 4, and 5 (infrared) are 3.55-3.93, 10.3-11.3 and 11.5-12.5 respectively. As in Durkee (1984), this study used channels 1 and 2 for analysis of aerosol features.

13

Channels 4 and 5 are used to indicate water vapor patterns and compute MCSST. Channel 3 data could not be used due to excessive noise. The time differences between NOAA-7 and aircraft measurements collected on the same day are 6 to 79 minutes. For more details on the NOAA-7 satellite and AVHRR sensor see NOAA Polar Orbiter Data Users Guide from the National Environmental Satellite, Data, and Information Service (Kidwell, 1984).

   2.   The Aircraft Measurement System

        The aircraft, a twin-engine Piper Navajo, flew in two distinct flight patterns to maximize the sampling density of the measurment region. One pattern was constant altitude legs, flown at different altitudes, to provide two-dimensional cross-sections of the region. The other was vertical spirals, to get high resolution samples through the air column. The aircraft normally flew with a 54 m/s airspeed during the measurement periods. With an 'on-station' flight time of about four hours, the aircraft could sample up to 800 km of airspace in one flight. The vertical spiral measurements were the only data analysed for this study.

        The aircraft was equipped to measure state variables as well as aerosol properties as described by Noonkester (1981). A listing of the aircraft instrumentation is given in Table I. The T, T_d, P, SST, ASSP, LWC and radiation flux measurements listed in the table were obtained continuously throughout the flights. The wand collections, CN and LIDAR measurements were made systematically at specific intervals during the flights.

        The PRT-5 measures SST over a 2° field of view (FOV) by combining radiances over a wide frequency band from 8 to 14 microns. The temperature accuracy is approximately $\pm 0.1^{\circ}$C.

```
                              TABLE 1
                      AIRCRAFT INSTRUMENTATION


State Variables:

     temperature, T - Rosemount sensor, HP Quartz sensor
     dew point, $T_d$ - EG and G cooled-mirror hydrometer
     static pressure, P - Rosemount sensor
     sea surface temperature, SST - PRT-5

Aerosol and Cloud Particles:

     size distribution - ASSP (Axially Scattering Spectrometer Probe),
                    0.23 - 14.7 μm radius particles
     particle composition - particle composition wand (Hobbs et al.,
                    1976)
     cloud liquid water, LWC - hot wire device (King et al., 1978)
     condensation nuclei, CN - rapid expansion counter (Hobbs et al.,
                    1976)

Radiometers and Lidar

     shortwave and longwave radiative flux - Eppley pyranometers, both
                                          up- and down-pointing
     1.06 μm LIDAR, down-pointing (Lentz, 1982)
```

B.   PROCEDURES AND DATA ANALYSIS

The procedures for data analysis started with converting AVHRR brightness counts to temperatures for channels 4, and 5. Then MCSSTs, calculated from channels 4 and 5, were compared to low altitude (30 to 60 m) and higher altitude (1000 to 1500 m) PRT-5 measurements. The location of these measurments were visually correlated with tropospheric aerosol concentration patterns calculated from a combination of channel 1 and 2 radiance values. Aircraft-measured environmental variables were used to investigate the changes

with altitude of PRT-5 SSTs. Also, radiance values, calculated by the LOWTRAN 6 model using the aircraft measured atmospheric profiles, were converted to temperatures and compared to the PRT-5 measured SST profile. Aerosol contributions were investigated by varying the LOWTRAN prescribed aerosol distribution. The changes of PRT-5 SST measurements with altitude are discussed in chapter three.

1. NOAA-7 AVHRR Data Analysis

The NOAA-7 AVHRR images were collected by the Scripps Satellite Oceanography Facility (SSOF). The image brightness counts from channels 4 and 5 were converted to temperatures using an algorithm described in Lauritson et al. (1979). These temperatures are then used to calculate and display MCSST.

The MCSST computations use a daytime MCSST equation derived by Strong and McClain (1984):

$$MCSST(daytime) = 1.0346T_4 + 2.58(T_4 - T_5) - 283.21, \qquad (2.1)$$

where T_4 is the brightness temperature in degrees K for channel 4, T_5 is the brightness temperature for channel 5 and the MCSST results are in degree C.

Channel 4 (11 μm) has a higher transmittance than channel 5 (12 μm) with respect to water vapor. Channel 5 is affected more by water vapor, which results in typically cooler temperatures as upwelling radiance is absorbed and reemitted through the atmosphere.

2. Environmental Data and Calculations

Air temperature (T), dewpoint temperature (T_d), pressure (P), sea surface temperature (SST) and altitude were measured directly by the aircraft. Relative humidity (RH), water vapor density (ρ_v) and potential temperature are calculated. The saturation vapor pressure, e_s, used to calculate relative humidity is defined by Tetens (1930) and

16

verified by Bolton (1980). Noonkester (1980) discusses the total errors accumulated in the RH calculation used for this study. The accuracies for the state variable sensors are: temperature (T), $\pm 0.1^\circ$C; dewpoint temperature (T_d), $\pm 0.5^\circ$C; and pressure (P), ± 1 mb. See Durkee (1984) for further details on computations of relative humidity, mixing ratios, vapor pressures, water vapor density, and potential temperature.

3. <u>Extinction Coefficient Calculation</u>

In a cloud-free marine environment the upwelling radiance is influenced primarily by two types of scattering. These are Rayleigh or molecular scattering which exists throughout the atmosphere and Mie or aerosol scattering which is usually confined to the marine boundary layer, especially in the presence of a subsidence-induced, low-level inversion.

Extinction coefficient values characterize the atmosphere's ability to absorb and scatter energy at specific heights. Applications and calculation of extinction are discussed as a basis for understanding the conclusions in chapter four.

Total upwelling radiance, measured at the top of the atmosphere, is a combination of emissions and reflections from the surface, transmittance, which is determined from extinction values, and the temperature profile through the air column as shown below (Liou, 1980),

$$I_\lambda = B_\lambda(T_s)T_\lambda(\infty,0) + \int_0^\infty B_\lambda(T(z))dT_\lambda(\infty,z), \qquad (2.2)$$

where the first term on the right hand side is the surface contribution to the total radiance and the second term is the atmospheric contribution. I_λ is the spectral upwelling radiance (watts $m^{-2}sr^{-1}/\mu m$). $B_\lambda(T_s)$ is the Planck function (watts $m^{-2}sr^{-1}/\mu m$), which relates emitted monochromatic intensity with frequency and temperature of the emitting substance, and is defined as:

17

$$B_\lambda(T) = (2hc^2) / \lambda^5(e^{hc/KT\lambda}-1),\tag{2.3}$$

where λ is the wavelength.

h is Planck's constant (6.6262×10^{-27} erg sec).

c is the velocity of light (2.99793×10^{10} cm sec^{-1}).

K is Boltzmanns' constant (1.3806×10^{-16} erg deg^{-1}).

T is absolute temperature.

$T_\lambda(\infty,z)$ is transmittance from a given height to the top of the atmosphere. When transmittance is weighted by the Planck function and summed through the atmosphere, as in the second right hand term, it yields the upwelling radiance contribution from the atmosphere. Since this term is dependant on temperature and extinction within each layer, it represents the atmospheric effect on the total upwelling radiance. Spectral transmittance is related to optical depth by the equation

$$T_\lambda(z) = e^{-\tau},\tag{2.4}$$

where τ is the optical depth and is calculated by:

$$\tau = \int_0^H \beta_{ext} dz.\tag{2.5}$$

The extinction coefficient (in units of per length) is defined by:

$$\beta_{ext} = \int_0^\infty \pi r^2 Q_{ext}(m,r) \ dN(r)/dr \ dr,\tag{2.6}$$

where Q_{ext} is the extinction efficiency of a particle with radius r and complex index of refraction (m), $dN(r)/dr$ describes the size distribution of the particles and, πr^2 is the cross-sectional area.

Durkee (1984) discusses the relationship between the terms of the extinction coefficient equation and shows that

for each set of values there is a bounded range of particle sizes which contributes to the extinction coefficient. With this information, data collection and analysis can concentrate on specific particle size ranges to get required information. The size distribution, N(r), was determined from the ASSP measurements aboard the aircraft. The extinction efficiency, Q_{ext}, was calculated from Mie theory and is a function of the complex index of refraction, wavelength (λ) and particle radius. The extinction values used for this analysis were calculated for the study by Durkee (1984), which used the same data set. The method of calculation is discussed in detail within that report. The extinction coefficients used in this study were computed at 0.63 μm, the median frequency of AVHRR channel 1.

C. LOWTRAN 6 SEA SURFACE TEMPERATURES

The PRT-5 SST value is a combination of optical depth and sea surface radiance contributions weighted over a wide frequency band of 8-14 microns. The type, amount and particle size of constituents in the air at any given time determine the value of optical depth. LOWTRAN 6 is used to investigate the contributions of individual constituents. LOWTRAN 6 is a model which computes atmospheric radiance and transmittance from either a model atmosphere or a measured atmospheric profile. Radiance can be calculated for many different combinations of parameters.

Comparing PRT-5 SST and model-generated SST indicates which constituents or parameters of the atmosphere have a major influence on the PRT-5 measurements. The weighting factor of each frequency used by the PRT-5 was unknown. Two frequencies were chosen for model computations (8 and 11 μm), so comparisons could be made between the model derived SSTs and PRT-5 SSTs. Transmittance at 8 μm is lower than at 11 μm due to water vapor and aerosols. For each frequency the model was run for two cases: one used the aircraft

measured atmospheric profile, including water vapor, but without the internal aerosol model of LOWTRAN 6; the second was the same profile with the internal aerosol model. Radiance was calculated first for the entire atmospheric column from the surface to the highest altitude of each vertical spiral and then from the surface to the next-to-the-highest altitude and so on through the final, lowest layer. LOWTRAN 6 limits the number of levels in the atmospheric profile to 34, so many of the top spiral altitudes used by the model are not the highest altitudes where the aircraft took measurements. The main area of interest extends from the surface to a few hundred meters above the marine boundary layer. This layer was included in all the atmospheric profiles used here.

The model radiance values were converted to SST by Planck's function (see Eqn. 2.3) in the form of:

$$T(^{\circ}K) = \frac{hc/K}{\lambda(\ln(2hc^2/\lambda^5(B_{\lambda}(T))),} \qquad (2.7)$$

where λ is the wavelength. The resulting model SST is compared to the PRT-5 measured SST to investigate atmospheric effects on SST measurements or infrared radiance.

III. RESULTS

Comparing aircraft-measured vertical profiles of aerosol extinction, air temperature, water vapor density and SST shows relationships between each component and it's contribution to infrared upwelling radiance. Atmospheric effects on aircraft measured radiance will also affect the radiance measured by the NOAA-7 satellite. A better understanding of contributions to atmospheric effects will lead to a more accurate satellite-derived SST. An atmospheric transmittance model, LOWTRAN 6, is used to show qualitatively how individual constituents, specifically aerosols and water vapor, contribute to the atmospheric effects on remotely sensed SST.

A. METEOROLOGY

Data to be analysed were collected on 21-22 September and 1 October 1982. A sub-tropical high dominated the southern California Coast on all three days. The associated subsidence was strongest on the 22nd as indicated by a shallow inversion layer. This stable layer traps ocean generated particles and is often topped with stratrocumulus, but not during this period. Fig. 3.1 shows the vertical profiles of potential temperature (θ), and relative humidity (RH) for spiral "A1" on 22 September. Note the constant θ and high RH layer from the surface to the top of the inversion at 155 m. A frontal system passed through the area on 26 September. By 1 October the inversion layer was reestablished. Due to increasing marine boundary layer mixing, the inversion layer deepened from 200 m on 1 October to 450 m on 5 October.

B. EXTINCTION PROFILES AND OPTICAL DEPTH

Extinction coefficients were calculated using 0.63 μm for 21 and 22 September, which gives the aerosol contribution to optical depth and, therefore, radiance. The particle size distribution measurements failed on 1 October, so extinction values could not be calculated.

The highest extinction values were found in the inversion layer with the largest value often near the top of the inversion, where relative humidity also reaches a maximum. The highest extinction value of 1.786 km^{-1} occurs at the inversion of spiral A1 from 22 September, depicted in Fig. 3.1. Table 2 contains a list of extinction values at the inversion. From the inversion level heights on 22 September, it appears that the mixing in the boundary layer at "A1" is still relatively strong compared to "B". Under the same high pressure system, the inversion height at "A1" is 155 m while at "B" it is 70 m. This may be attributed to the fact that SST at "A1" is $0.4^{o}C$ warmer than at "B". The warmer SST contributes to instability within the boundary layer which generates mixing through the boundary layer.

The optical depths listed in Table 2 were calculated by summing 25 extinction values from aircraft measurements taken at a minimum altitude of 35 m and a maximum of 1209 m. The optical depth values are not directly comparable, since they are for air columns of different height. However, by examining the profiles of extinction, air temperature and water vapor a relationship between the measured SST and optical depth can be determined. When the extinction contribution to the atmospheric term in Eqn. 2.2 for upwelling radiance is understood, then similar conclusions can be drawn from the sum of extinction values or optical depth.

On 21 and 22 September the air temperature profiles have a minimum value at the top of the marine boundary layer, and
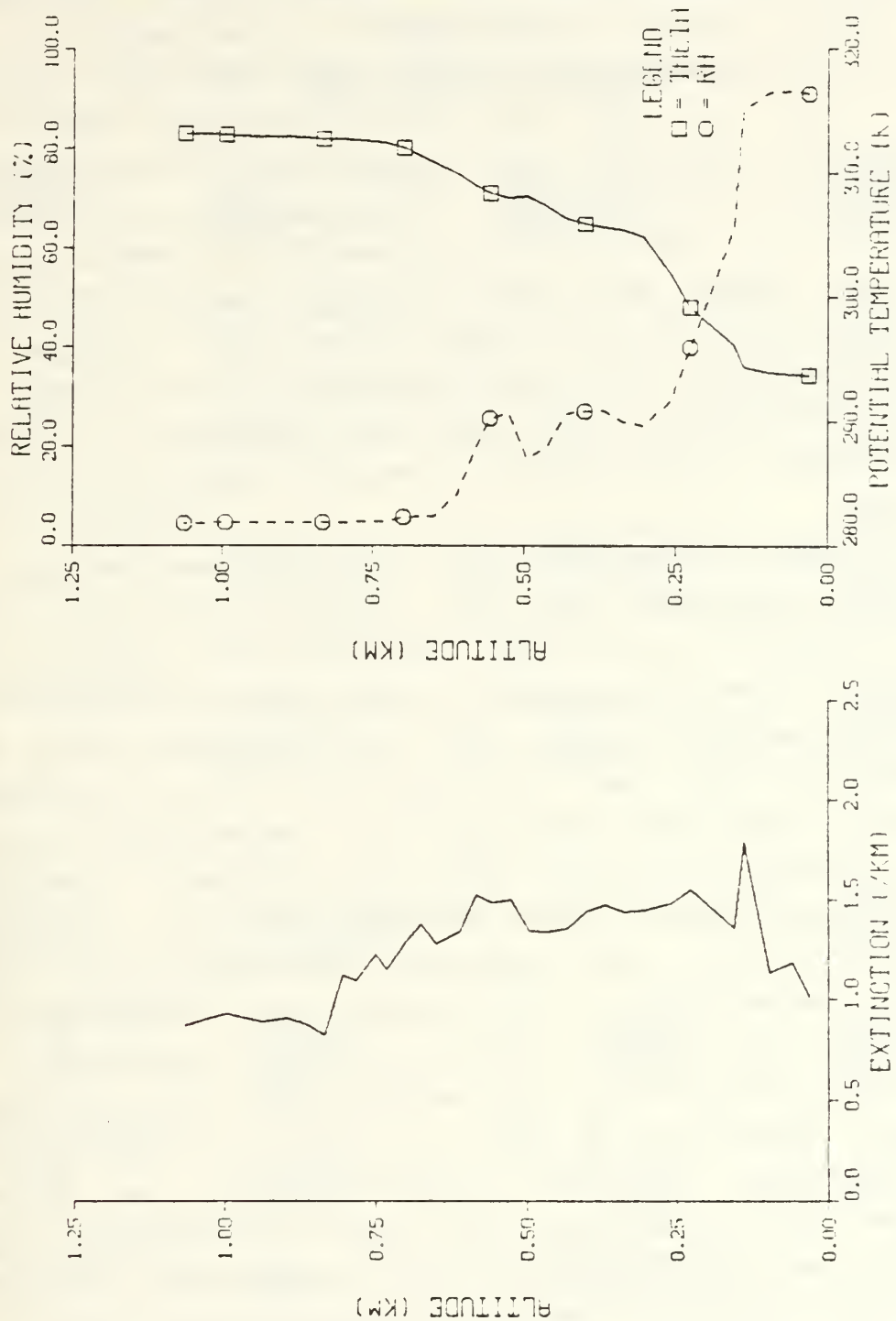
Figure 3.1   Calculated extinction, relative humidity
and potential temperature from the vertical spiral
measurements at point A1 on 22 September 1982.

23

temperature increases above the boundary layer. The water vapor profile shows a high, uniform concentration in the marine boundary layer and then decreases above the boundary layer. Fig. 3.2 shows the air and dewpoint temperature profiles and water vapor density and PRT-5 SST measurements for spiral A1 on 22 September. Note the close relationship between the air temperature and measured SST, even with high extinction values above the boundary layer. The high extinction produces low transmittance which reduces the upwelling radiance. The air temperature is warm enough so that any reduction of the upwelling radiance by reduced transmittance is not enough to keep the measured SST from increasing.

On 21 and 22 September, the PRT-5 SST measurements at each spiral decreased from the surface to the top of the marine boundary layer and then increased with altitude. In each spiral, the SST measured at the top of the spiral by the PRT-5 (maximum height 1000 m.) was warmer than the temperature at the lowest altitude by 0.4 to 0.7 degrees. This can be explained using Eqn. 2.2. Radiance has contributions from both the surface and the atmosphere. Normally, the upwelling radiance should decrease with height if transmittance decreases and temperature decreases. At lower altitudes, especially in the boundary layer where aerosol density and water vapor density are high, extinction is high. This results in a high optical depth and low transmittance. Therefore, by Eqns. 2.2 and 2.5, the optical depth increases, and the radiance from the surface decreases. On 22 September, below the marine boundary layer where the temperature decreased and transmittance decreased with height, radiance or measured SST decreased. This is in agreement with Eqn. 2.2. The minimum PRT-5 SST was at the top of the boundary layer where the air temperature reached a minimum and transmittance was the lowest. Above the

24

TABLE 2

SPIRAL SEA SURFACE TEMPERATURES AND OPTICAL DEPTHS

Date/Spiral	Spiral Alt(m): Top/Inversion/Bottom	PRT-5 SST(C): Top/Inversion/Bottom	Average MCSST/Deviation
21 Sep 1982			
B	1000/160/26	20.24/19.53/19.79	19.55/ -0.22-+0.15
AB	917/160/36	20.13/19.44/19.62	19.78/ -0.25-+0.17
A1	942/160/42	20.00/19.44/19.49	19.64/ -0.06-+0.31
B1	923/200/36	20.14/19.41/19.63	20.15/ -0.06-+0.31
22 Sep 1982			
B	873/70/51	20.19/19.49/19.57	19.78/ -0.14-+0.13
B1	907/98/57	20.75/19.97/19.99	20.37/ -0.21-+0.15
A1	804/155/31	21.33/19.81/19.96	20.78/ -0.15-+0.26
01 Oct 1982			
B	1209/185/36	18.66/18.89/19.21	18.83/ -0.27-+0.47
B1	940/200/34	18.70/18.73/19.00	18.75/ -0.11-+0.30

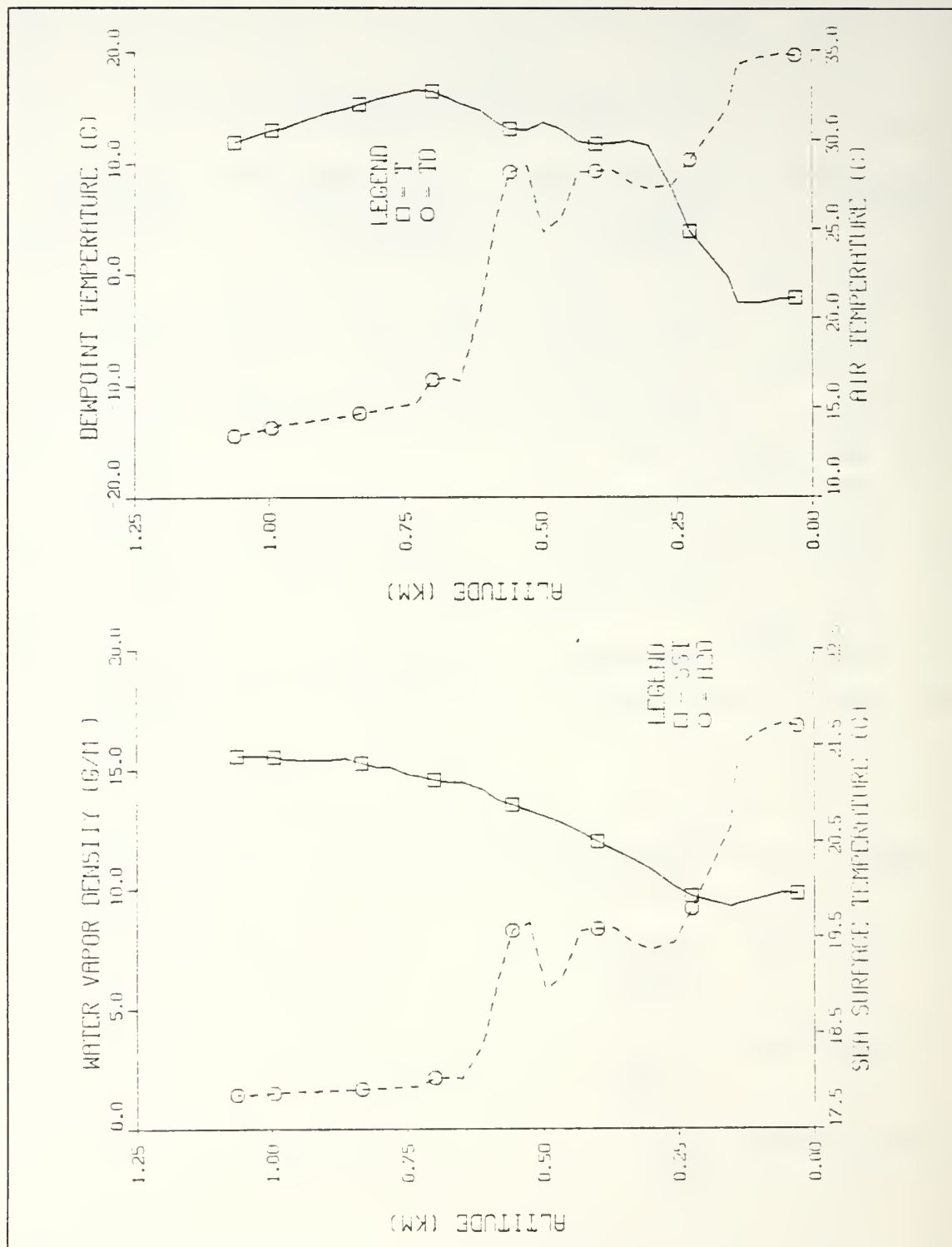| Date/Spiral	Extinction(km^{-1}): At Top of Inversion	Optical Depth	ΔSST MCSST - Bottom
21 Sep 1982			
B	1.0590	.5785	-0.24
AB	1.1833	.5283	+0.16
A1	1.1323	.6086	+0.15
B1	0.7316	.3221	+0.52
22 Sep 1982			
B	1.7128	1.057	+0.21
B1	1.6102	1.018	+0.38
A1	1.7864	1.360	+0.82
01 Oct 1982			
B	Not	Available	-0.38
B1	Not	Available	-0.27

Figure 3.2   Aircraft measured values of sea surface
temperature, air and dewpoint temperature and water
vapor density at point A1 on 22 September 1982.

26

boundary layer, the rise in air temperature increased the atmospheric contribution to upwelling radiance and, therefore, increased the PRT-5 SST measurement. The total transmittance continued to decrease with altitude but not enough to cool or offset the warming air temperature's effect on the radiance.

On 1 October 1982, extinction was not calculated because of the lack of particulate data, but the response of the PRT-5 measurements can be discussed in terms of the atmospheric term of Eqn. 2.2 A marine boundary layer is evident by the minimum air temperature at the top of the layer and a fairly constant potential temperature, especially in spiral B1 as shown in Fig. 3.3. The air temperature increased above the boundary layer and then decreased with height. Water vapor density was highest in the boundary layer, decreased rapidly above the boundary layer then gradually decreased with height. The PRT-5 SST measurement reached a minimum at the top of the boundary layer. Again, this may be attributed to the minimum in air temperature and decreased transmittance from the surface. Above the boundary layer, the PRT-5 measured SST increased slightly then decreased with height.

Comparing air temperature, water vapor density, and measured SST profiles from 21 and 22 September and 1 October can indicate to what degree each contituent contributes to the atmospheric effects. Within the marine boundary layer, the 21 and 22 September profiles had higher air temperatures, water vapor density and relative humidity than on 1 October. As a result of higher atmospheric contributions from higher temperature and water vapor density, the resulting PRT-5 SST measurements are higher on 21 and 22 September than on 1 October. Though the general values are lower on 1 October the trends of each profile are similar within the boundary layer. The air temperature reached a
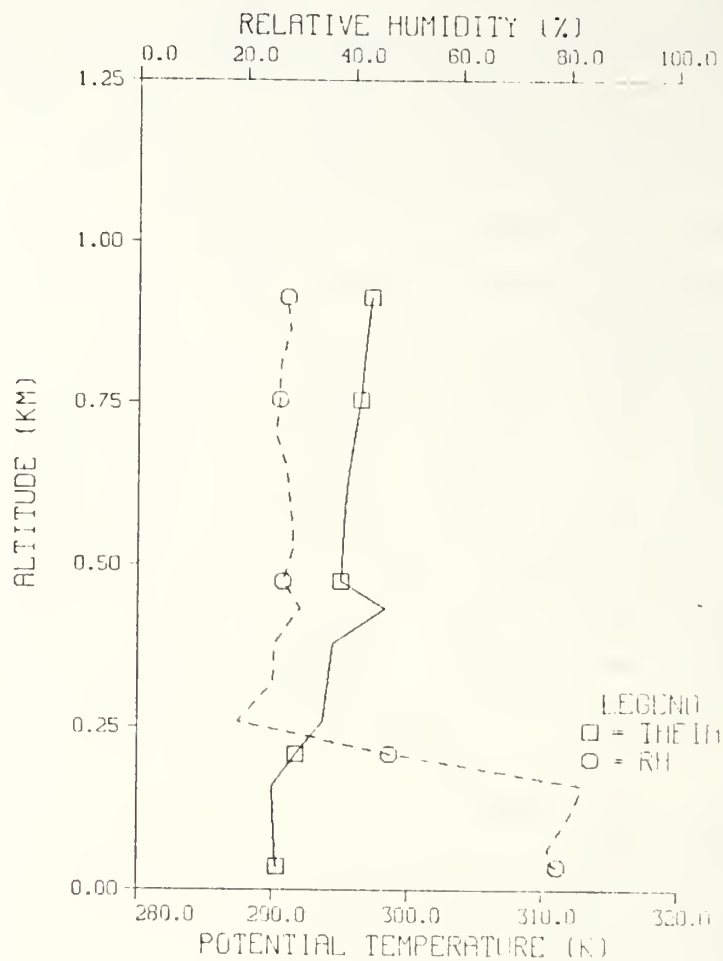
27

Figure 3.3   Calculated values of relative humidity
and potential temperature from the vertical spiral
measurements at point B1 on 1 October 1982.

28

minimum at the top of the boundary layer, while water vapor density, relative humidity and, therefore, aerosol size reached a maximum.

Above the boundary layer, 21 and 22 September air temperature profiles were warmer than 1 October and increased with height. The air temperature on 1 October increased for a few meters above the boundary layer then decreased with height. The water vapor density and relative humidity profiles on 22 September indicate that this was the driest atmosphere above the boundary layer of the three days. The 21 September profile had a moist layer between 600 and 800 m. Otherwise the water vapor profile was similar to that of 1 October. The measured SST increased with the height of measurement on 21 and 22 September. On 1 October, measured SST increased for about the first 50 m above the boundary layer, and then it decreased with height. Above the boundary layer, the temperature had the major influence on the atmospheric effect to upwelling radiance. On 22 September, the aerosol transmittance was not low enough to offset or cool the increased radiance due to the temperature increase. On 21 September, the aerosol transmittance seems to offset the increased air temperature effects, because the measured SST was not increasing with height as much as on 22 September. Because the air temperature profiles were generally cooler on 21 September than on 22 September the aerosol extinction was high enough to offset or decrease the measured upwelling radiance. This resulted in smaller differences of measured SST values on 21 September than on 22 September. On 21 September the SST differences of the highest minus the lowest altitude measurements, ranged from +0.45 to +0.53 degrees. On 22 September they ranged from +0.59 to +1.37 degrees. On 1 October, the highest SST measurements were cooler then the lowest measurements by 0.26 to 0.38 degrees. This may have been caused solely by

decreasing air temperatures or by a combination of decreasing air temperatures and extinction by aerosols. Without the extinction profiles the aerosol contribution is unknown.

C. COMPARISON OF SATELLITE DERIVED AND PRT-5 SST

Values of extinction by aerosols have a distinct effect on PRT-5 measurements. To link satellite detected SST accuracy with any aerosol effects, a comparison is made between the lowest altitude PRT-5 measurement and MCSST. Table 2 shows PRT-5 SST measurements at the bottom and top of the spirals and average MCSSTs.

On 21 September, the difference between the MCSST and bottom PRT-5 SST measurement are small, ranging from -0.24 to +0.52 degrees. This indicates that the aerosol optical depth had offset increased upwelling radiance due to increased air temperature. On 21 September, the air temperature profiles at all four spirals were similar. As seen in Table 2, the MCSST-minus-lowest-altitude SST value is highest (+0.52) at spiral B1 where the optical depth is the lowest (.3221). At "B1", the optical depth was not high enough to offset the increase in upwelling radiance due to increased air temperature. The MCSST at "B1" is closer to the PRT-5 measured SST at the top of the spiral, showing that aerosol optical depth and vertical temperature profiles must be considered when calculating a satellite-derived SST.

On 22 September, the SST difference is the largest (0.82°) at spiral A1, where optical depth and air temperature values were the highest. This spiral also had one of the lowest altitude PRT-5 measurements (31 m). This implies that the increase in upwelling radiance due to the increasing air temperature was not offset or reduced by the low aersol transmittance for this spiral.

On 1 October 1982, the SST differences were very small. In both spirals the PRT-5 SST was warmer than the MCSST. At

"B" the PRT-5 SST was warmer by 0.38 degrees and at "B1" by 0.26 degrees. The decrease in air temperature with height decreased the upwelling radiance which was sensed by the satellite, making it cooler than the actual temperature. Analysis by Durkee (1984) indicates that aerosol contribution should have been considerably lower on 1 October due to a frontal passage on 26 September.

There are some considerations that must be remembered while comparing the MCSST and PRT-5 measured SST:

- The PRT-5 measurement is not at the surface. The lowest altitude for PRT-5 measurements range from 26 to 57 m, and this may be significant because of the high water vapor, relative humidity and aerosol content within the boundary layer. The actual SST is probably warmer than measured at a higher altitude since the decrease in air temperature and transmittance would reduce the radiance.

- The angle of the radiometer to the ground is not constant due to aircraft orientation. This means that the radiometer is looking through different amounts of atmosphere which may have different transmittance values.

- The MCSST is an average of SSTs over approximately a 5 pixel square or 5 square kilometers. It is not a measurement directly below the lowest altitude PRT-5 point. The deviation of MCSST over the 5 square km at each spiral ranges from - 0.25 to + 0.31.

The MCSST equation seems to take "normal" marine aerosol concentration and temperature distribution into account. If there is a higher than normal air temperature profile which is not offset by aerosol optical depth, such as in spiral A1 on the 22nd, the MCSST is too warm. More studies have to be conducted to provide a broader basis for this finding and also in the reverse situation of a cooler than normal temperature profile for an area with and without aerosol optical depth contributions.

D. LOWTRAN 6 RESULTS- AEROSOL CONTRIBUTION

The PRT-5 measured infrared radiance over a wavelength range of 8 to 14 μm. Since the extinction values were calculated at 0.63 μm, the degree of aerosol effect to the PRT-5 SST measurements only can be assumed. Within LOWTRAN

6, radiance can be computed for any wavelength. An internal "Navy Maritime" aerosol model is an option in LOWTRAN 6 so radiance can be calculated with or without prescribed aerosol effects. Aerosol contributions are examined by using the LOWTRAN 6 radiance computations, both with and without the model aerosol distribution.

LOWTRAN 6 computes the atmospheric radiance using specified atmospheric parameters. For this study, four cases are examined. Two cases use two wavelengths (8 and 11 μm) without an aerosol profile from the LOWTRAN 6 model. Two other cases use the same two wavelengths with the LOWTRAN 6 Navy Maritime aerosol profile. As inputs to the aerosol model, all four cases use the aircraft atmospheric measurements, and the calculated water vapor density. Surface winds were obtained from daily San Nicolas Island soundings. San Nicolas Island soundings are shown in Appendix C.

On 21 September , the PRT-5 SST appears to be an average between SSTs calculated at 8 and 11 μm above the boundary layer, as seen in Fig. B.1 through Fig. B.4. Below the marine boundary layer the 8 μm profile without aerosols matches the PRT-5 SST measurements very closely at spiral A1 (See Fig B.3). This implies that at this spiral position, water vapor and decreasing temperatures below the boundary layer had a major influence on the PRT-5 measured SST. At spiral B1, there was additional cooling which may have been due to aerosol extinction. The model aerosol distribution lowered the model-computed SST, at 8 and 11 μm, to a greater degree than the PRT-5 SST profile at each spiral. The actual concentration and size of aerosol particles in the marine boundary layer of each spiral may be less than the model distribution, which would not decrease the measured radiance as much as the model.

The model aerosol concentrations are high in the marine boundary layer, and reduce rapidly above the layer. The

model-computed SST with aerosols was much cooler above the marine boundary layer than the PRT-5 SST. This shows that air temperature and water vapor are the major contributors to the PRT-5 SST profile above the marine boundary layer. The actual aerosol distribution above the boundary layer is higher than the model predicts. This means that while aerosols decrease the measured upwelling radiance they may also emit energy, thereby limiting the decrease of upwelling radiance as indicated by LOWTRAN calculated values. More cases have to be investigated using the LOWTRAN model and actual aerosol distributions to examine emission by aerosols. The shape of the PRT-5 SST profile is closely related to the 8 μm profile, which has lower transmissivity in the presence of water vapor than at 11 μm. This confirms that water vapor is a major influence on remotely sensed radiance.

The 22 September results are similar to those on 21 September. The significant result for this day is at spiral A1. There are identical profiles below the boundary layer of the PRT-5 SST and the model computed SST at 8 μm with aerosols (See Fig. B.7). Since these profiles did not match without the model aerosol distribution, this shows that aerosol had a pronounced effect in these conditions. Spiral A1 had the highest extinction value at the top of the marine layer and the highest total optical depth. The resulting low transmittance combined with the decreasing air temperature within the boundary layer decreased the measured radiance. This results in a minimum SST measurement at the top of the boundary layer.

Above the boundary layer, the model aerosol extinction decreased the measured upwelling radiance significantly. This indicates that when there are sufficiently high extinction values, the aerosols may also be emitting instead of only scattering.

On 1 October, the PRT-5 SST still appears to be an average of 8 and 11 µm, but whereas the 8 µm profile was generally warmer on the 21st and 22nd than 11 µm, it is now cooler. This is due to the much cooler air temperature and decrease in relative humidity, so that there are smaller radius aerosol particles emitting energy at 8 µm. The general shape of the PRT-5 SST profile again follows the 8 µm profile. Introducing aerosols into the model did not change the SST profiles computed at 8 and 11 µm without aerosols. The two profiles are nearly identical, indicating that the aerosol sizes and/or quantity are not large enough to affect the measured upwelling radiance. In the boundary layer, the relative humidity was less than on 21 and 22 September so the aerosols were most likely smaller. The smaller aerosols contributed less to attenuation and decreased the measured SST. Therefore, the air temperature and water vapor density were the major factors for measured SST on 1 October.

IV. CONCLUSIONS

The purpose of this study was to investigate the marine aerosol effect on satellite-derived SST. The initial step examined the effects of aerosol optical depth on upwelling radiance or SST measured by an aircraft mounted radiometer (PRT-5). The amount of aerosol contribution to upwelling radiance was examined using an atmospheric transmittance model, LOWTRAN 6. To apply these results to satellite-derived SST, PRT-5 measured SSTs were compared to satellite-derived SSTs. The satellite-derived SST was calculated from NOAA-7 channels 4 and 5 using a daytime multichannel sea surface temperature (MCSST) equation by Strong and McClain (1984). Data for this study were collected on 21 and 22 September and 1 October 1982 off the southern California coast. There was a frontal passage on 26 September which changed the environmental profiles between 22 September and 1 October.

Overall, the aerosol optical depth offset or decreased measured infrared radiance. On 21 and 22 September, within the marine boundary layer, the combination of decreasing air temperature with height and high aerosol extinction values resulting in low transmittance gave a minimum SST at the top of the boundary layer. This is in agreement with the upwelling radiance equation 2.2. LOWTRAN 6 also demonstrated for 21 and 22 September, especially for spiral A1 on 22 September, that aerosols decreased model-calculated SST within the boundary layer. On 1 October, within the boundary layer, the PRT-5 measured SST did reach a minimum at the top of the boundary layer. On this day aerosol extinction values were not available but analysis by Durkee (1984) indicated that the aerosol contribution should have been considerably lower on 1 October due to a frontal

35

passage on 26 September. From the comparatively low relative humidity values and LOWTRAN 6 results, the minimum SST at the top of the boundary layer is due to the water vapor content and minimum air temperature value. When model aerosol distribution was added to LOWTRAN-calculated SST for 1 October, the SST profile did not change from the case without aerosols.

Above the boundary layer, on 21 and 22 September, the air temperature increased with height which increased the atmospheric term and, therefore, the upwelling radiance. The total measured upwelling radiance depends on how much the aerosol optical depth decreased the radiance. On 21 September, the aerosol optical depth offset the increase in air temperature so that the PRT-5 SST difference between those measured at the top and bottom of the spiral are smaller than those on 22 September. On 21 September, the top PRT-5 SST measurement was 0.45 to 0.53 degrees warmer than those measured at the lowest altitude. On 22 September, the top PRT-5 SST measurement was 0.59 to 1.37 degrees warmer than those measured at the lowest altitude. The larger difference on 22 September demonstrates that with high aerosol extinction, measured radiance will depend on the aerosol extinction offset of the air temperature effects on radiance. On 1 October, the air temperature above the boundary layer increased for about 50 m then decreased with height. The PRT-5 SST followed the same pattern as the air temperature. The top SST measurement is 0.26 to 0.38 degrees cooler than the SST measured at the lowest altitude. On this day the measured radiance decreased with height due to a decrease in temperature. The aerosol effect is not known but can be assumed to be small from the LOWTRAN results.

Aerosols scatter, absorb, and emit radiant energy. The LOWTRAN aerosol distribution has high concentrations in the

marine boundary layer and reduces to a very small value above the boundary layer. On 21 and 22 September, using the measured atmospheric data profiles and model aerosol distribution, the model-calculated SST was much cooler than the actual PRT-5 profile. Above the boundary layer, the actual aerosol amount was higher than the LOWTRAN model amount. With a higher aerosol extinction the measured PRT-5 SST should be cooler than the model calculated SST. Since it is not cooler, this suggests that aerosols emit some radiant energy and does not decrease the measured radiance as much as the pure scattering process. Further aerosol data collection and analysis, along with atmospheric transmittance calculations with actual aerosol extinctions, are required to provide enough information to thoroughly investigate aerosol emittance.

Aerosol optical depth affects satellite-derived SST in the same manner that it affects PRT-5 measurements. On 21 and 22 September, the MCSST was more accurate where increased upwelling radiance due to increasing temperature was offset by scattering effects of aerosols. The MCSST-minus-the-lowest-altitude SST values on 21 September were generally small, ranging from -0.24 to +0.52 degrees. The largest difference (+0.52) occured at spiral B1 with the lowest aerosol optical depth. In this case, scattering by aerosols did not offset the increasing air temperature contribution to the radiance. On 22 September, the MCSST is warmer than the SST measured at the lowest altitude of the spiral, by 0.21 to 0.82 degrees. The largest difference (0.82) occured at spiral A1 where the aerosol optical depth was not high enough to offset the air temperature contribution to the upwelling radiance. On both dates, at the spirals with the largest SST difference between the MCSST and lowest altitude PRT-5 SST, the MCSST more closely matched the PRT-5 SST measured at the top of the spiral. On

1 October, the MCSST also more closely matched the SST value measured at the top of the spiral. This was not due to the aerosol effects as on 21 and 22 September since the aerosol contribution to upwelling radiance was small on 1 October. The decreased radiance due to the decreasing air temperature was not fully corrected for in the MCSST equation.

The MCSST equation seems to correct for "normal" marine aerosol concentrations and air temperature distributions. If there is a higher than normal air temperature increase and the aersol optical depth can not offset it, such as in spiral A1 in 22 September, the MCSST is too warm. Additional aerosol and environmental data collection and analysis are required to quantify the effects of aerosol optical depth on measured upwelling radiance.

A correction to the daytime MCSST equation (Eqn. 2.1) could be made by using a weighting factor from channels 1 and 2. On 21 and 22 September, the measured aerosol optical depths corresponded well with the pattern of aerosol concentration derived from a combination of channel 1 and 2 radiance values. The usefulness of this method was demonstrated by Griggs (1983) and Durkee (1984). To make any corrections, further data collection, plus analysis of existing data are required. Quantitative studies of aerosol optical depth, water vapor amounts and temperature profiles and how they affect the differences between satellite derived SST and "actual" surface SST, are also needed. In addition, the constant altitude flight data from the experiment described here should be analyzed for confirmation of the results of this study.

This study demonstrates that aerosol optical depth has a significant effect on infrared radiance and, therefore, measurements of SST. The presence of aerosols reduces the upwelling radiance, but the degree of the reduction is dependant on the air temperature profile. Satellite

measurements of aerosol optical depth, water vapor and vertical temperature can be used in correcting MCSST equations once the relationship between the environmental factors and the radiative transfer problem is understood.

APPENDIX A
SPIRAL MEASUREMENTS

This appendix contains figures of the vertical spiral measurements collected on 21-22 September and 1 October 1982, off the coast of southern California.
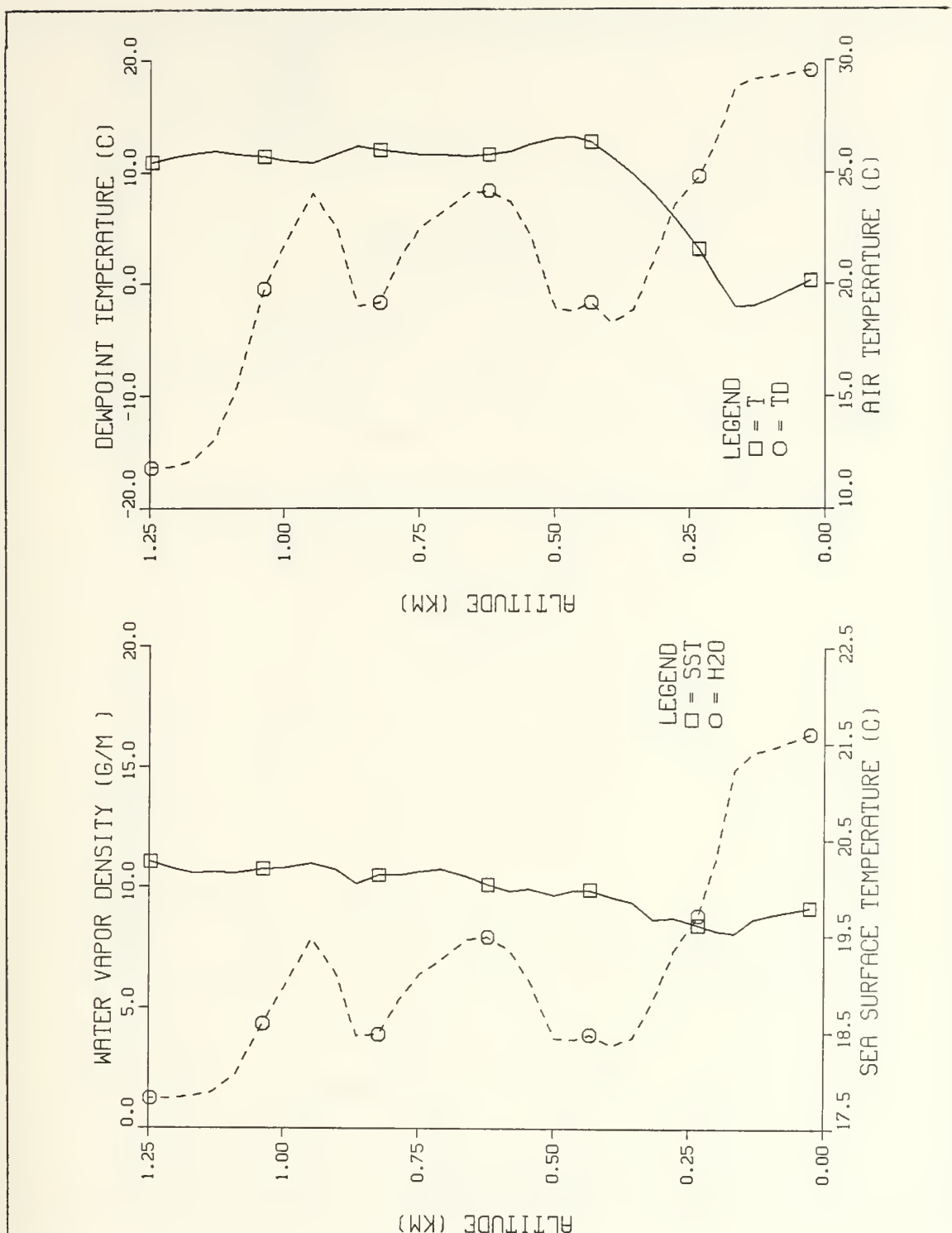
Figure A.1   Aircraft measured values of sea surface
temperature, air and dewpoint temperature and water
vapor density at point B on 21 September 1982.

41
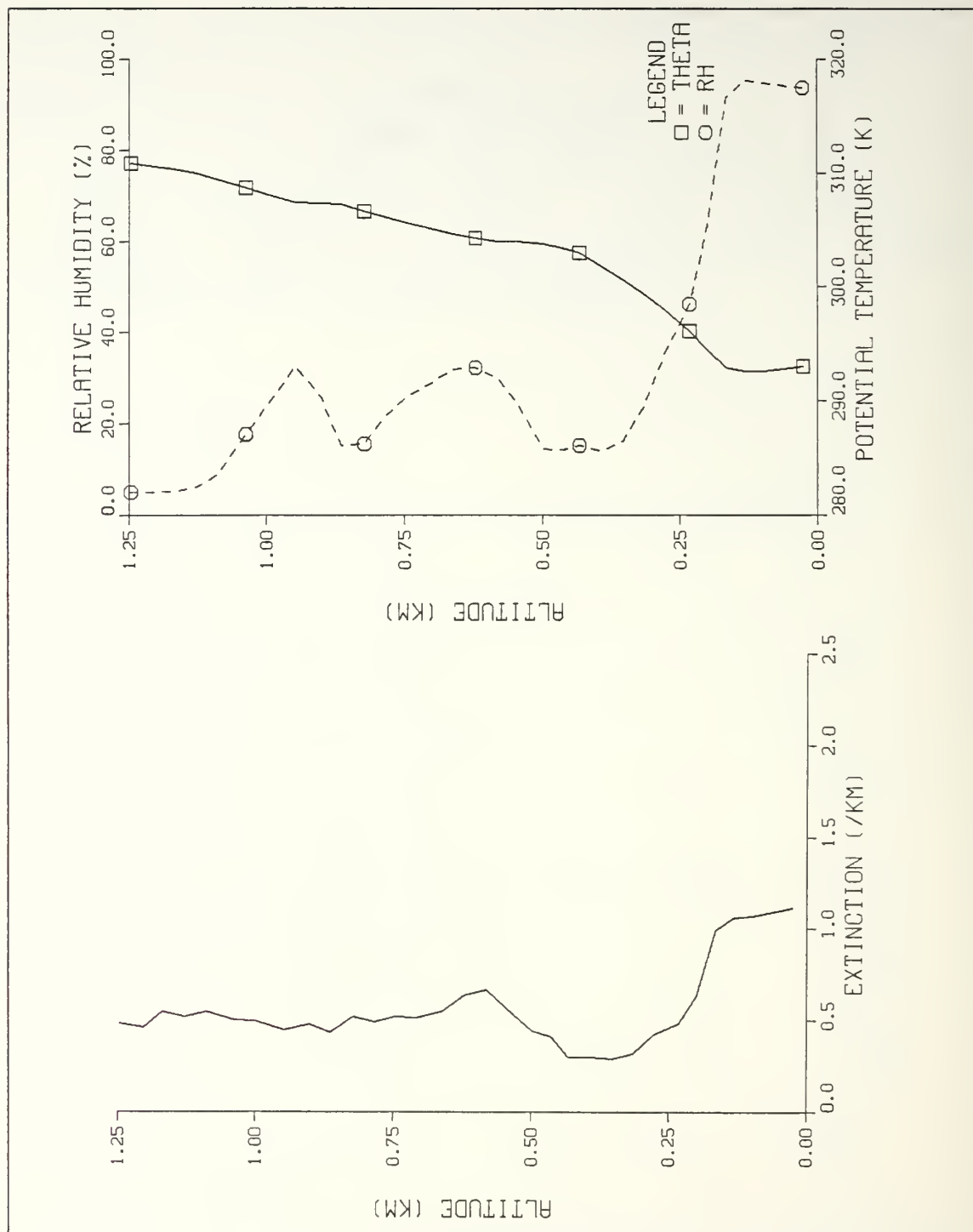
Figure A. 2   Calculated values of extinction, relative
humidity, and potential temperature from spiral
measurements at point B on 21 September 1982.
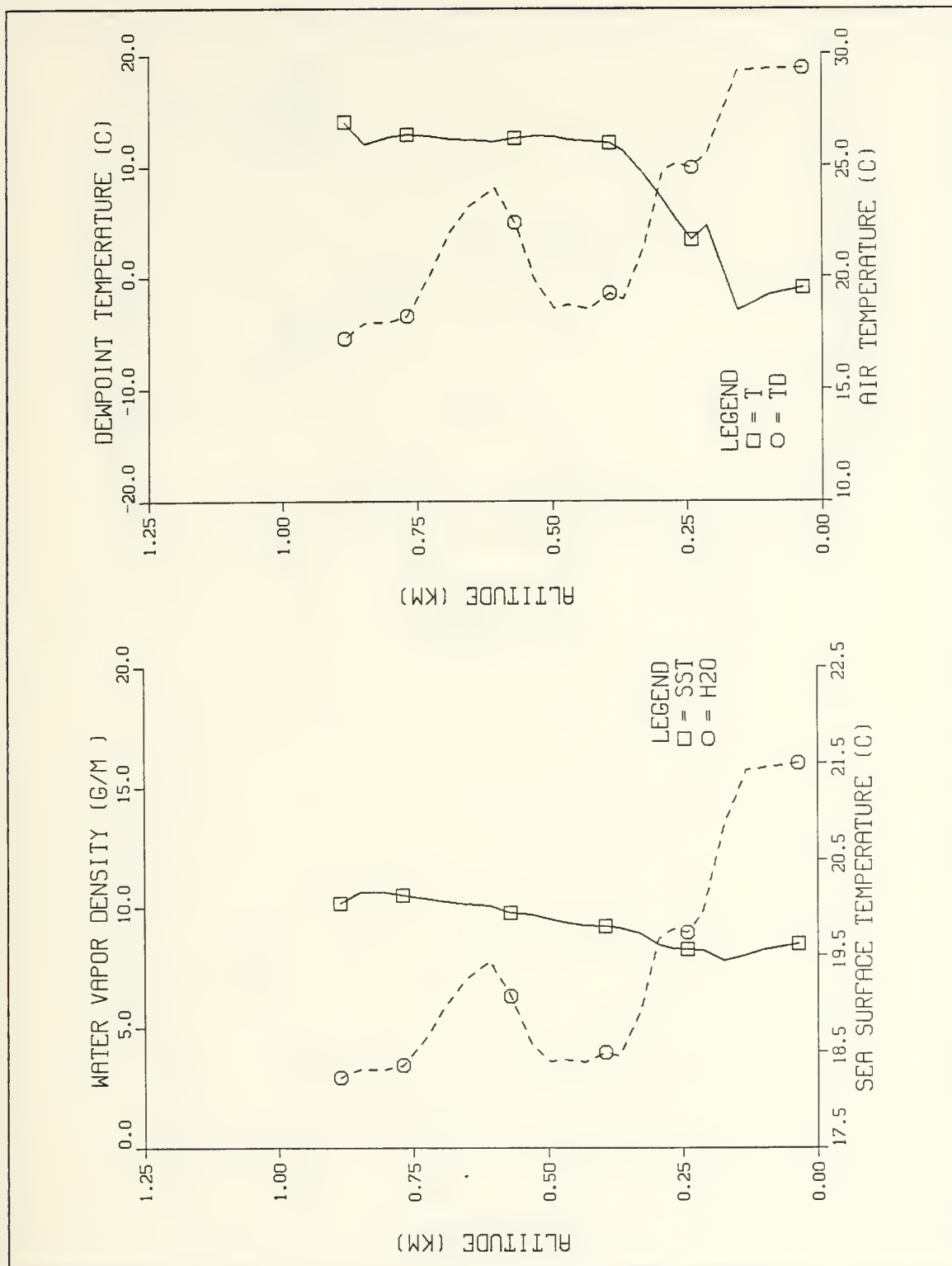
Figure A.3   Same as Fig. A.1 but for AB on 21 Sept 1982.
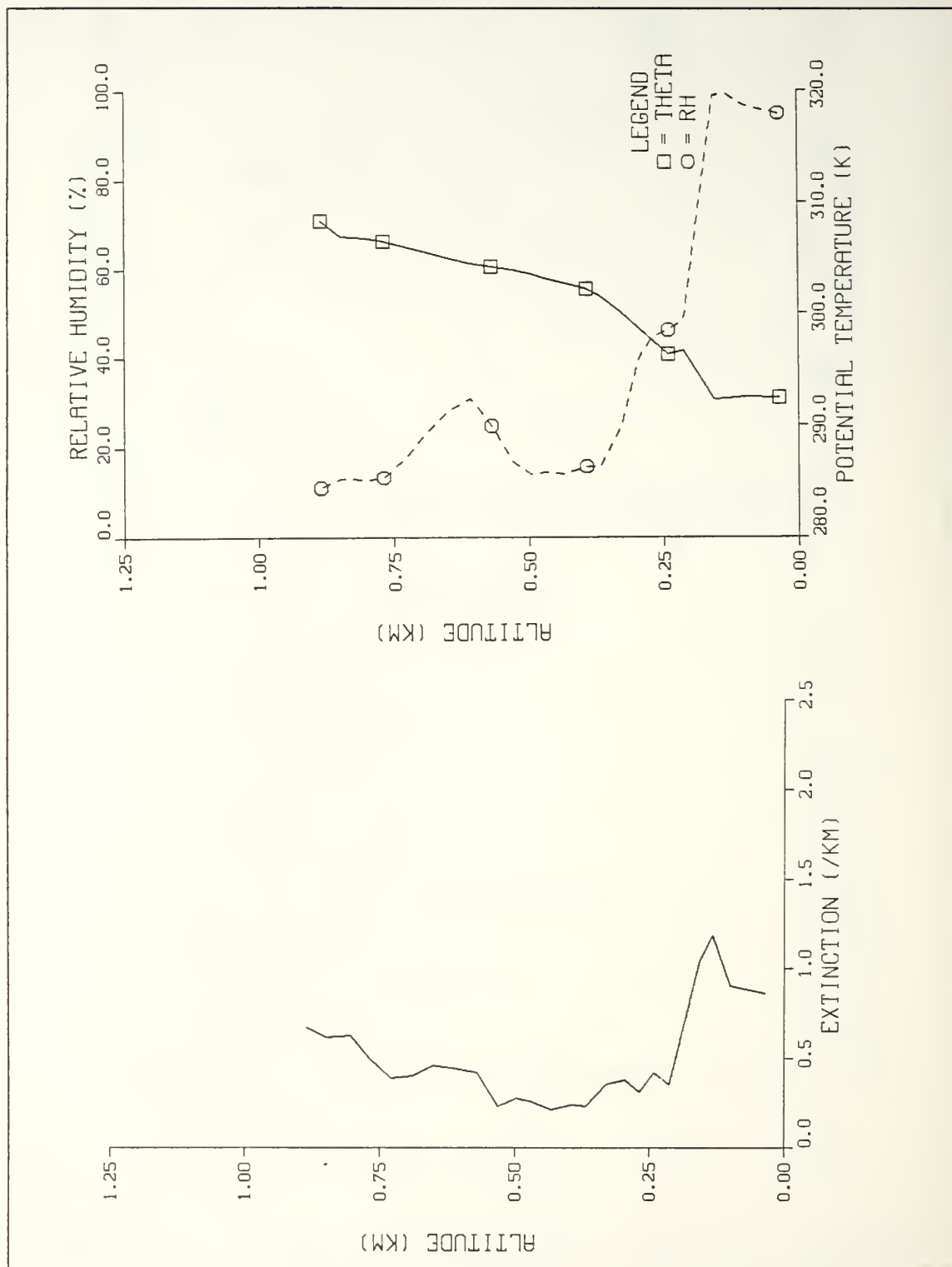
Figure A. 4   Same as Fig. A. 2 but for AB on 21 Sept 1982.
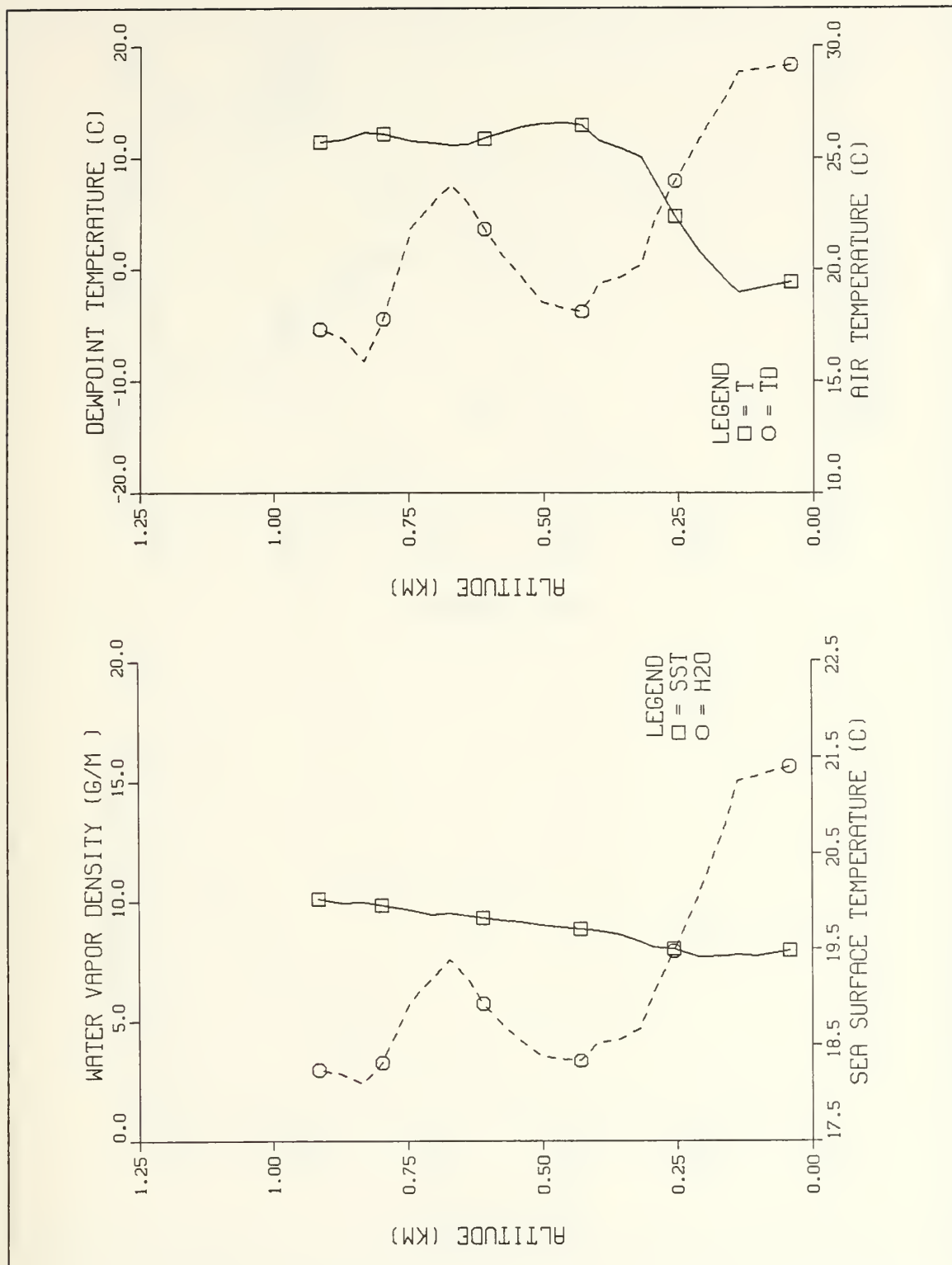
Figure A.5   Same as Fig. A.1 but for A1 on 21 Sept 1982.
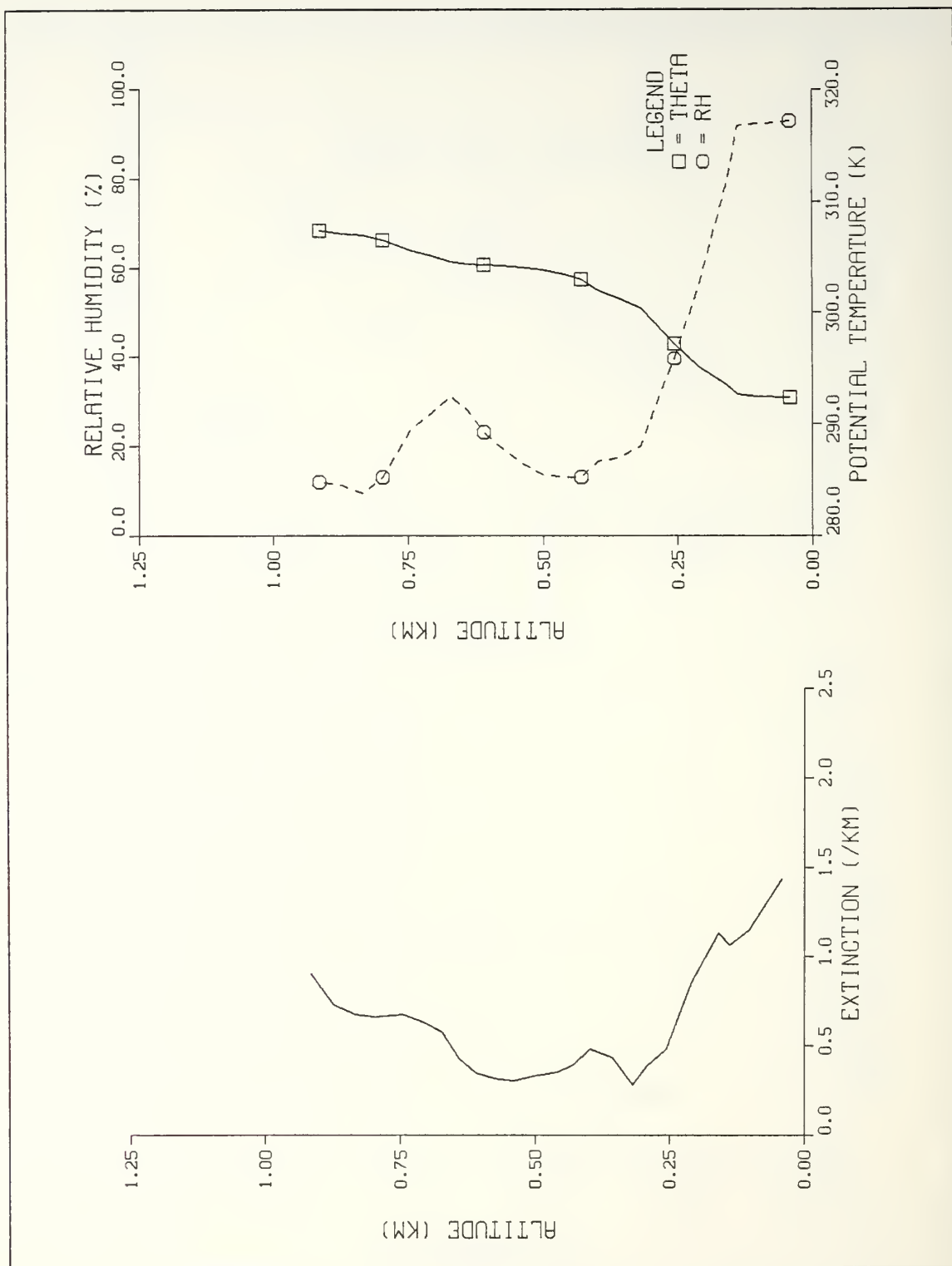
Figure A. 6   Same as Fig. A. 2 but for A1 on 21 Sept 1982.
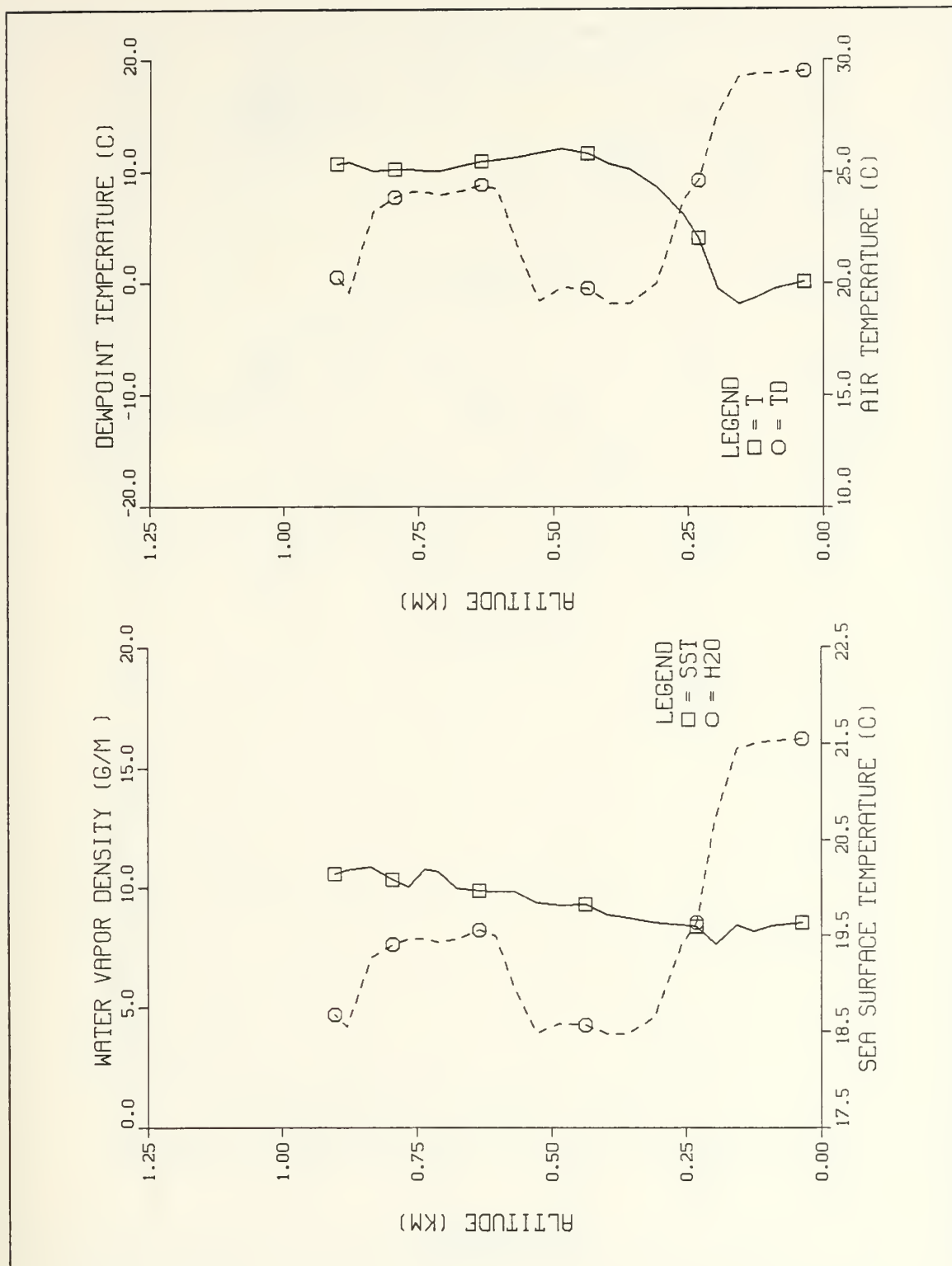
Figure A.7   Same as Fig. A.1 but for B1 on 21 Sept 1982.

47
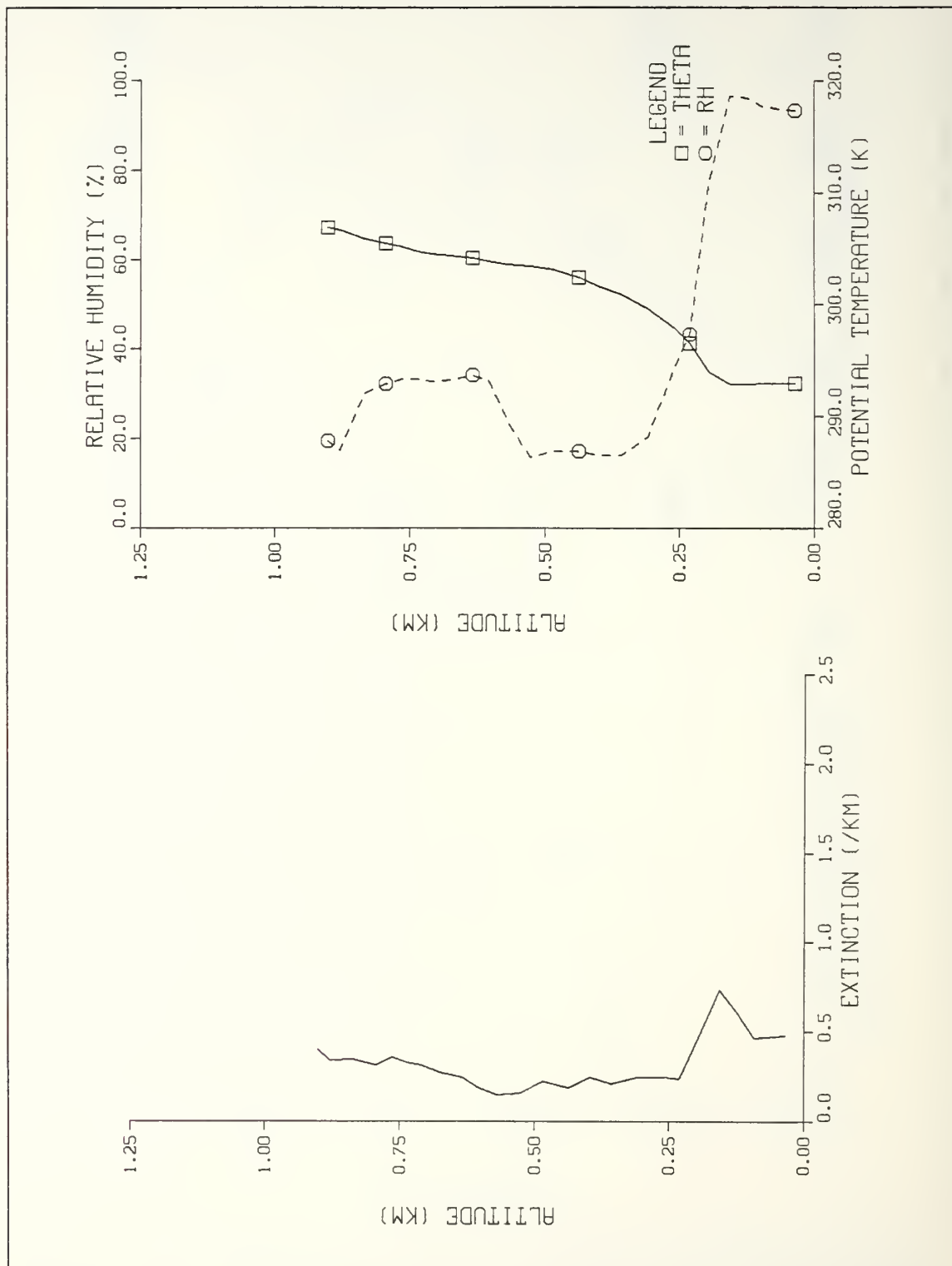
Figure A.8   Same as Fig. A.2 but for B1 on 21 Sept 1982.
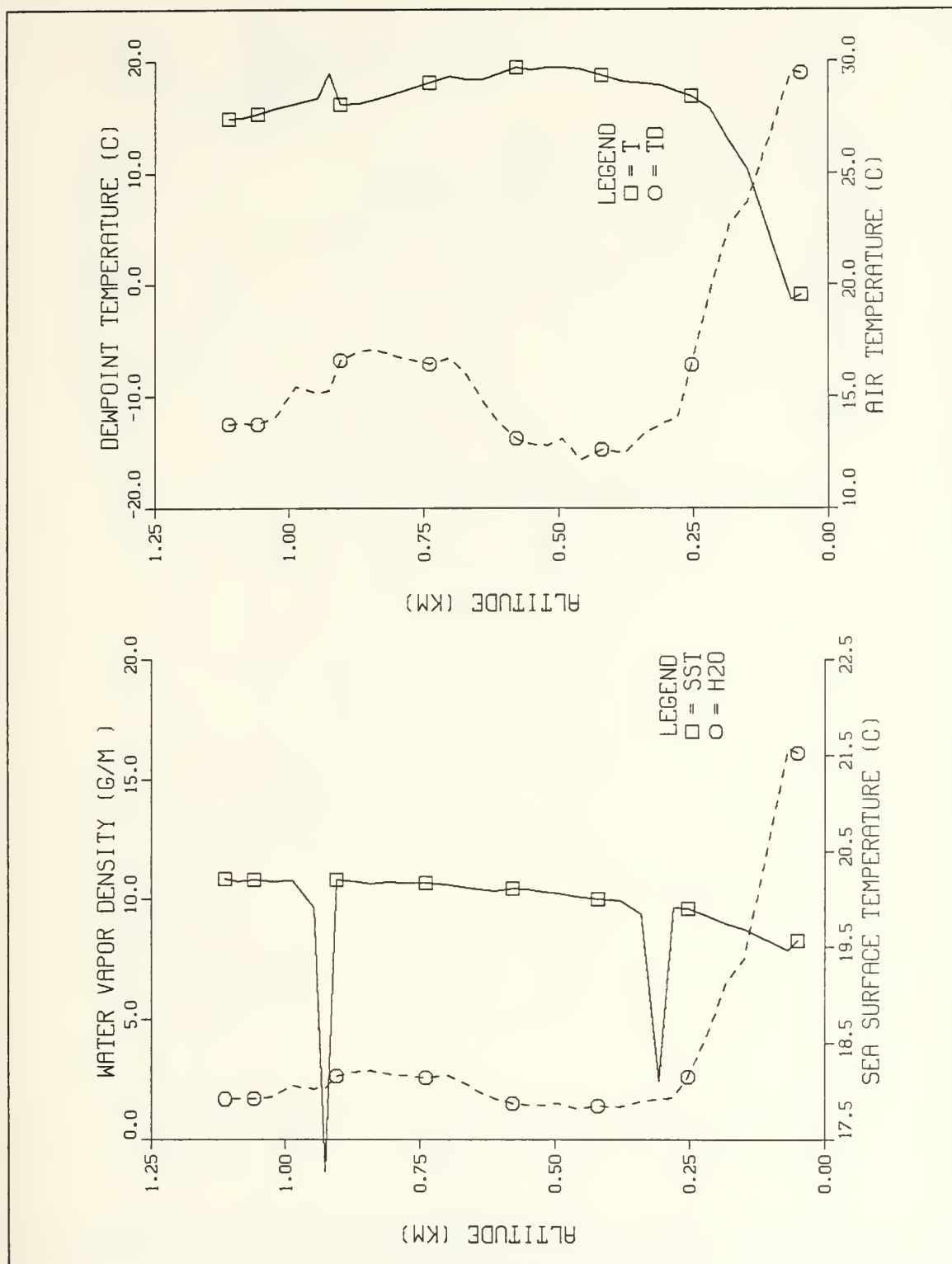
Figure A.9   Same as Fig. A.1 but for B on 22 Sept 1982.

49
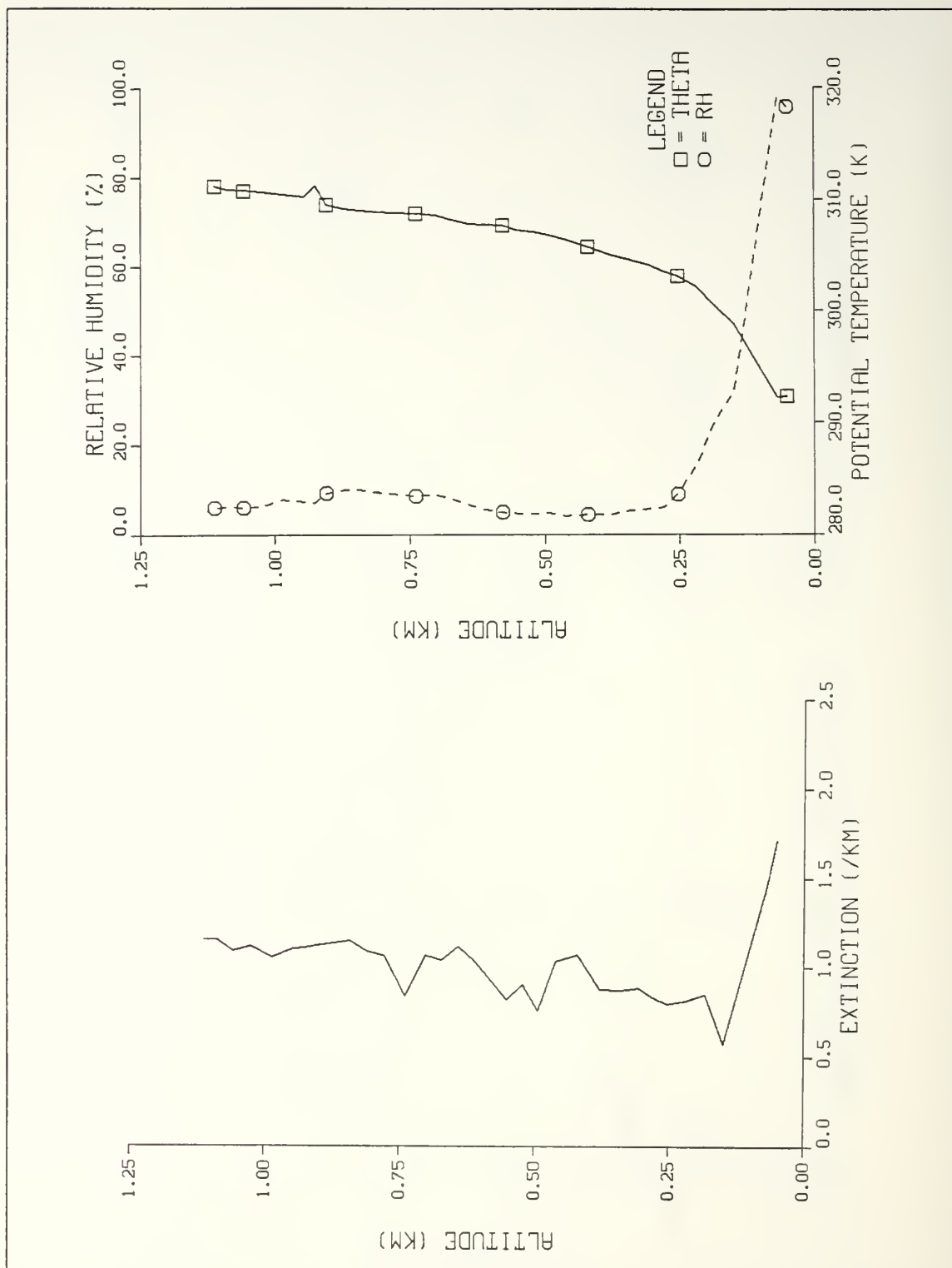
Figure A. 10   Same as Fig. A. 2 but for B on 22 Sept 1982.
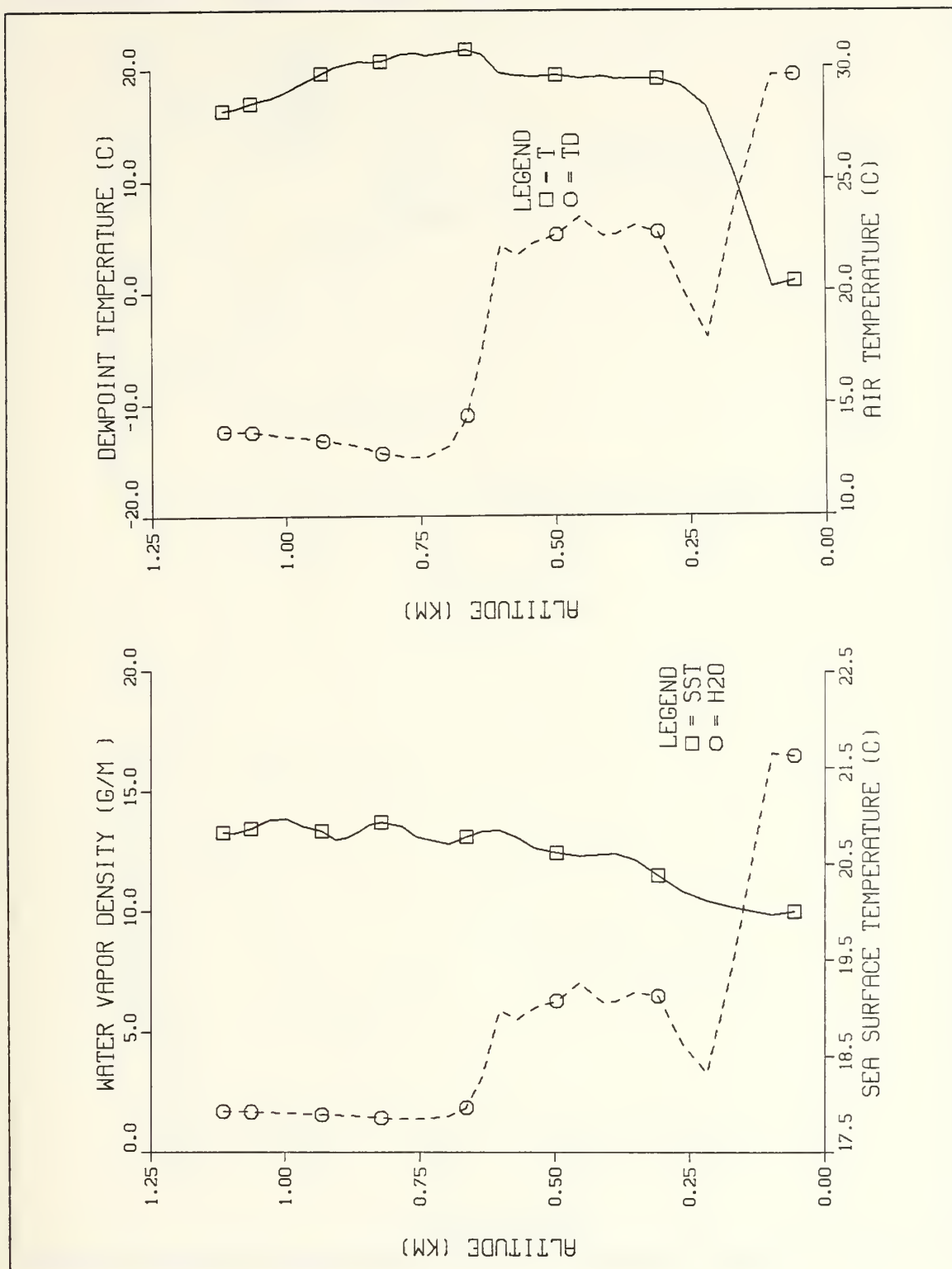
Figure A.11   Same as Fig. A.1 but for B1 on 22 Sept 1982.
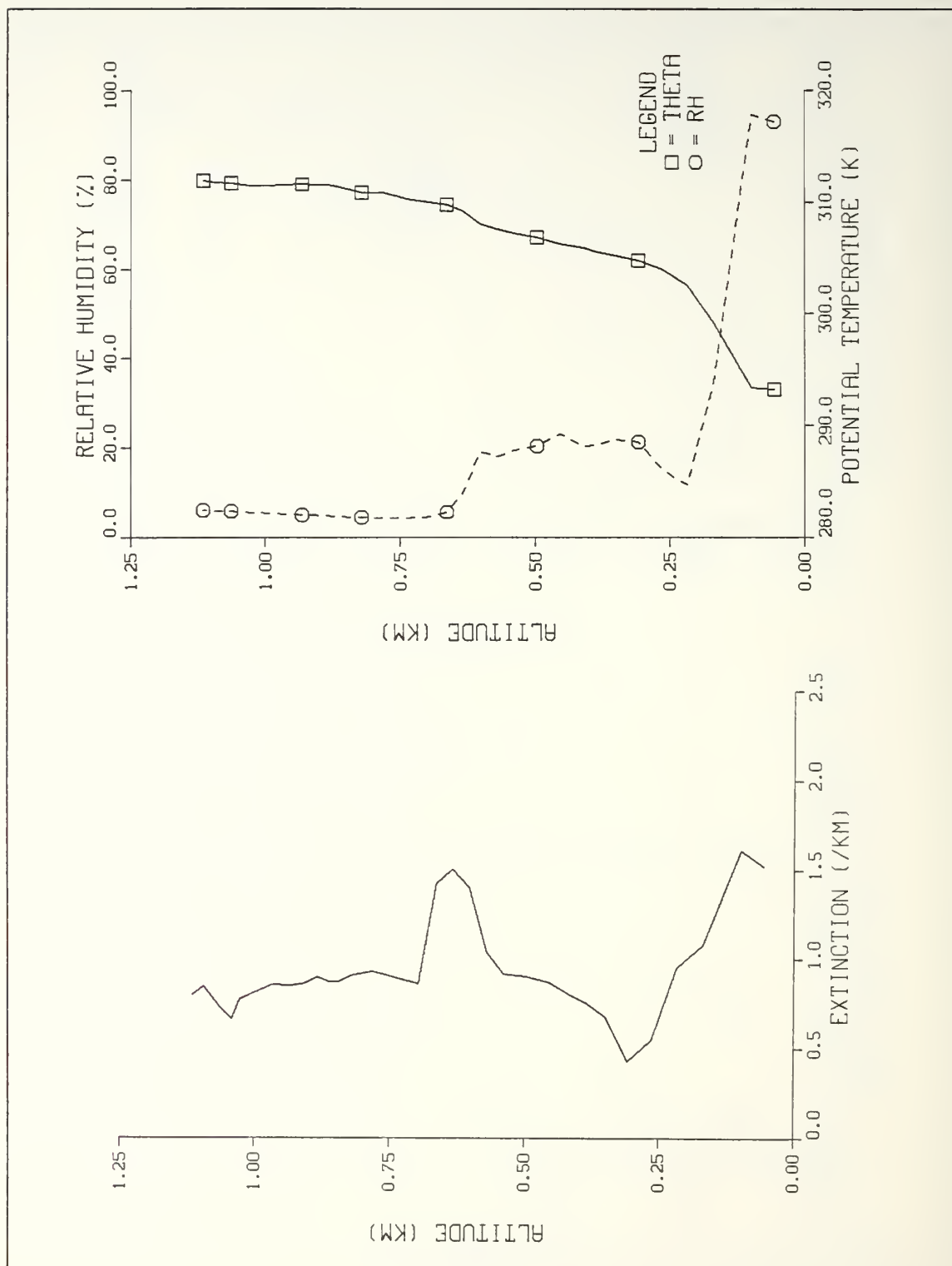
Figure A.12   Same as Fig. A.2 but for B1 on 22 Sept 1982.

52
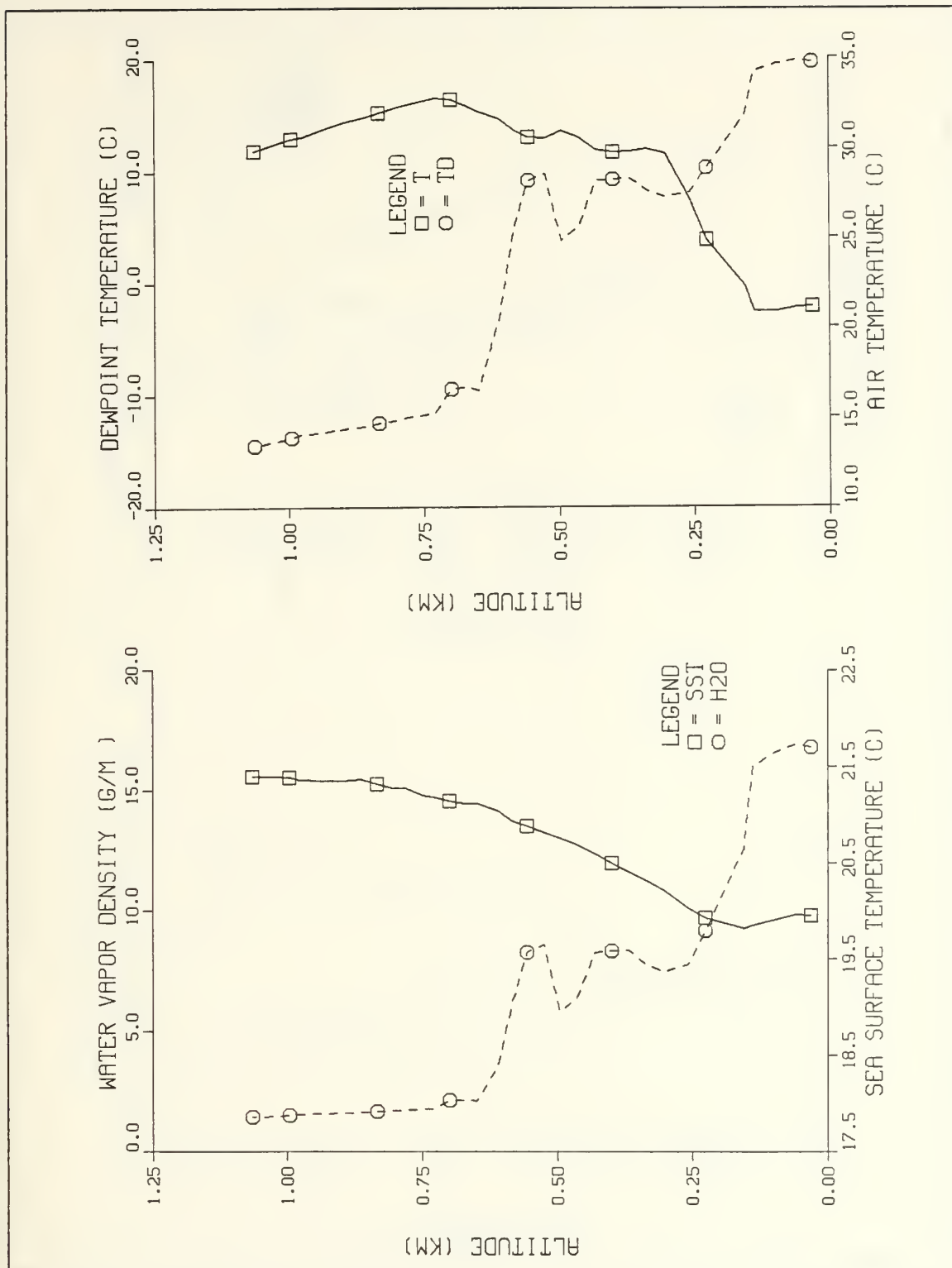
Figure A.13   Same as Fig. A.1 but for Al on 22 Sept 1982.
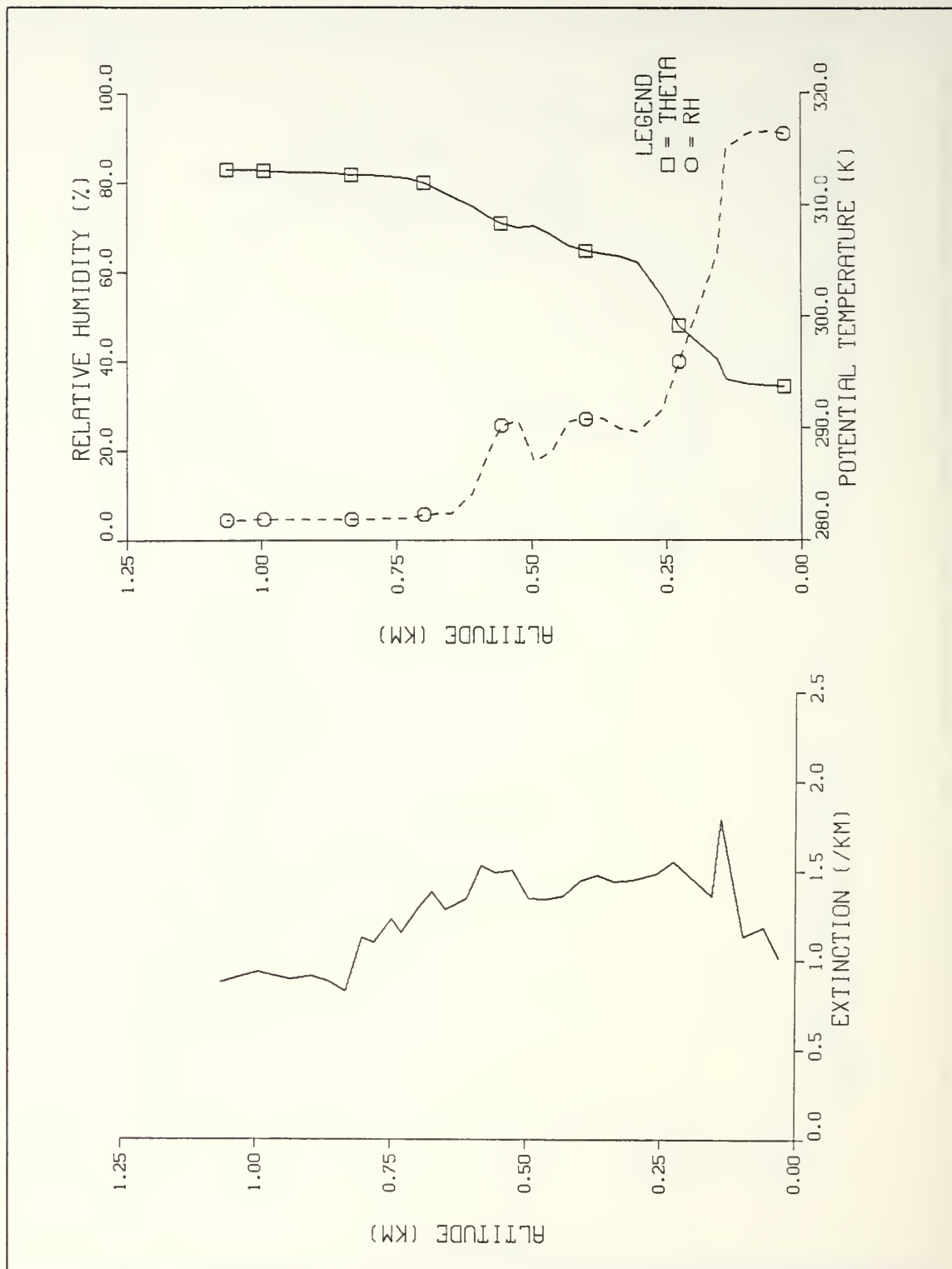
Figure A. 14   Same as Fig. A. 2 but for A1 on 22 Sept 1982.

54
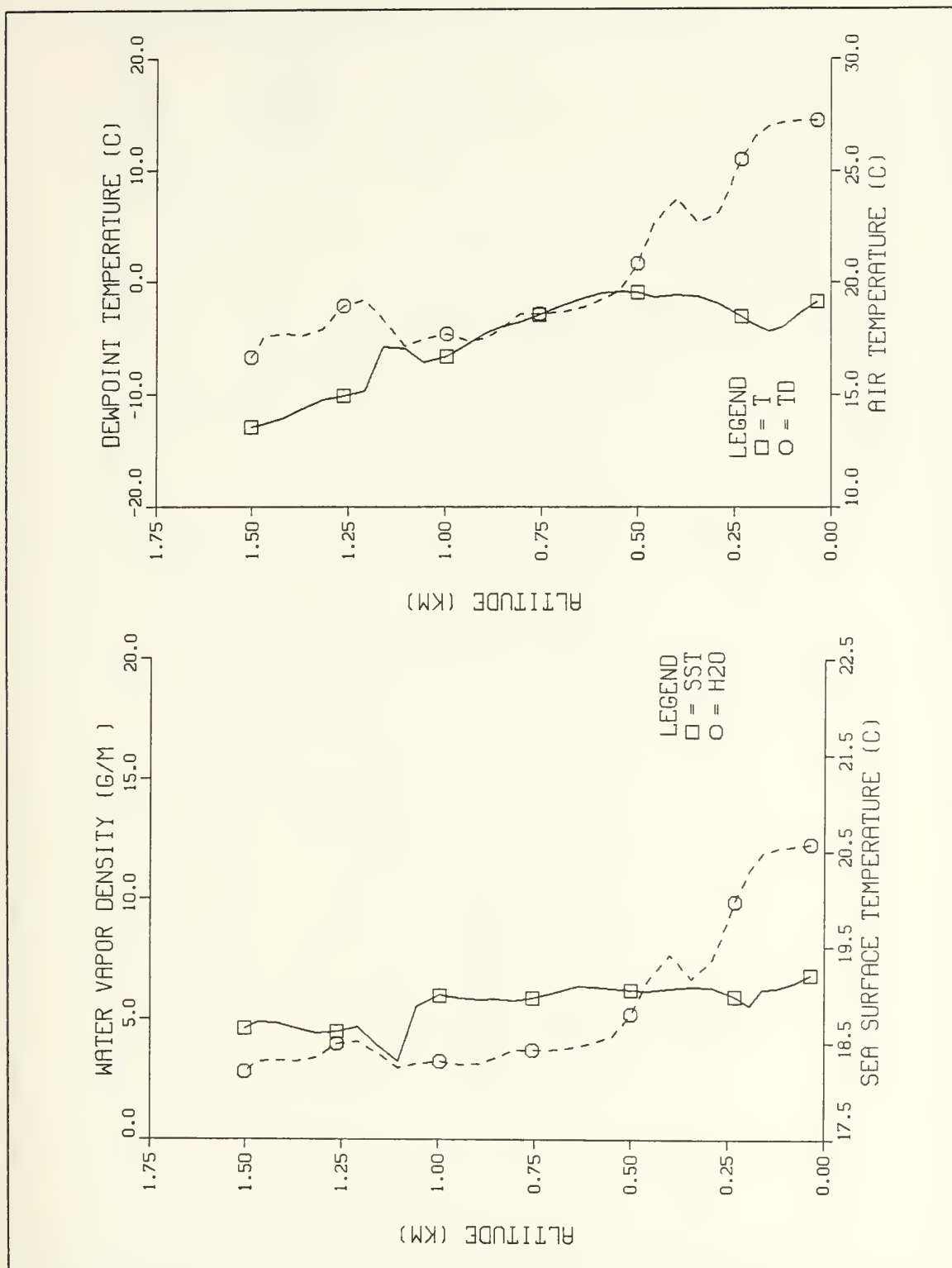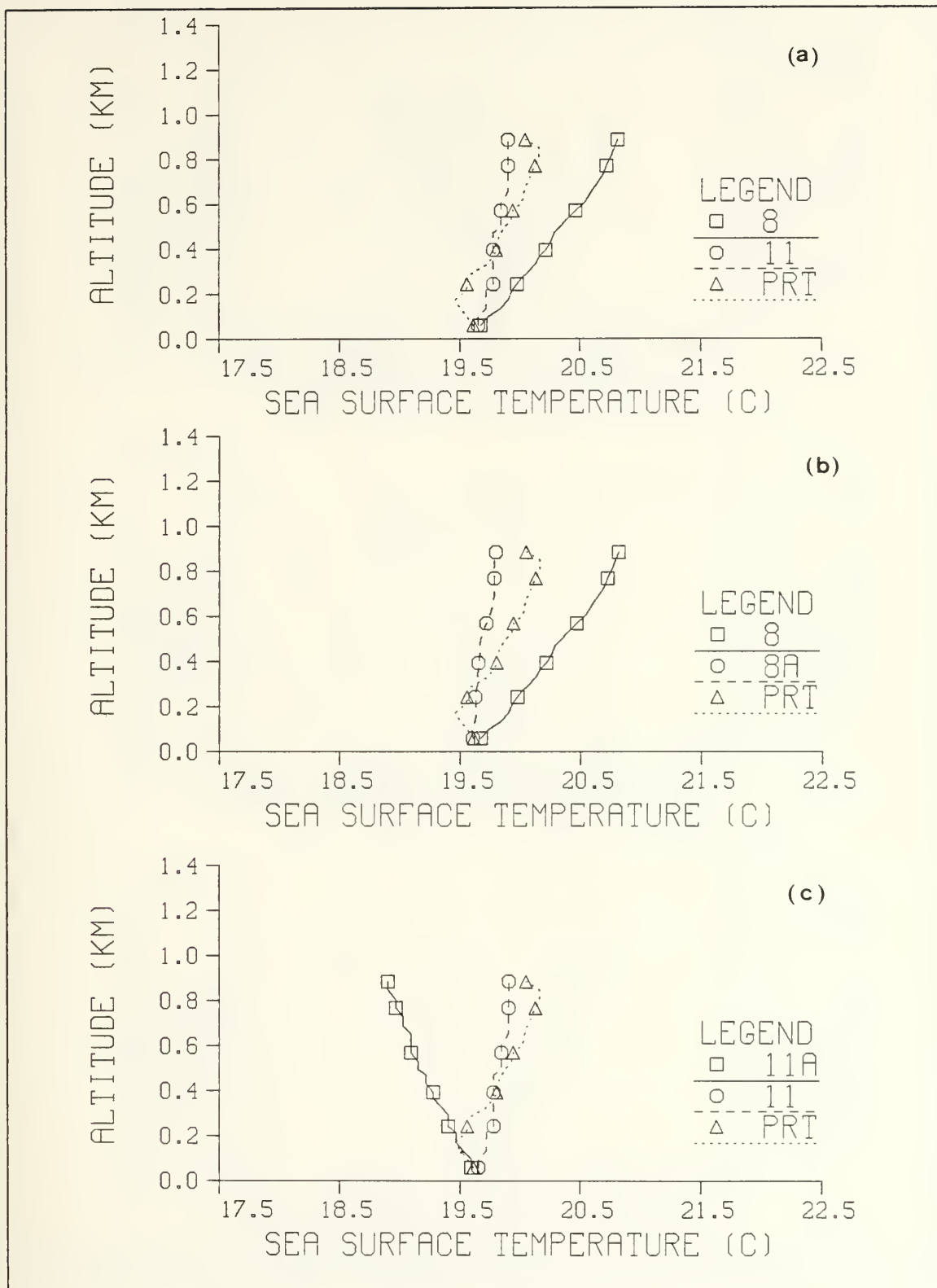
Figure A.15   Same as Fig. A.1 but for B on 1 Oct 1982.
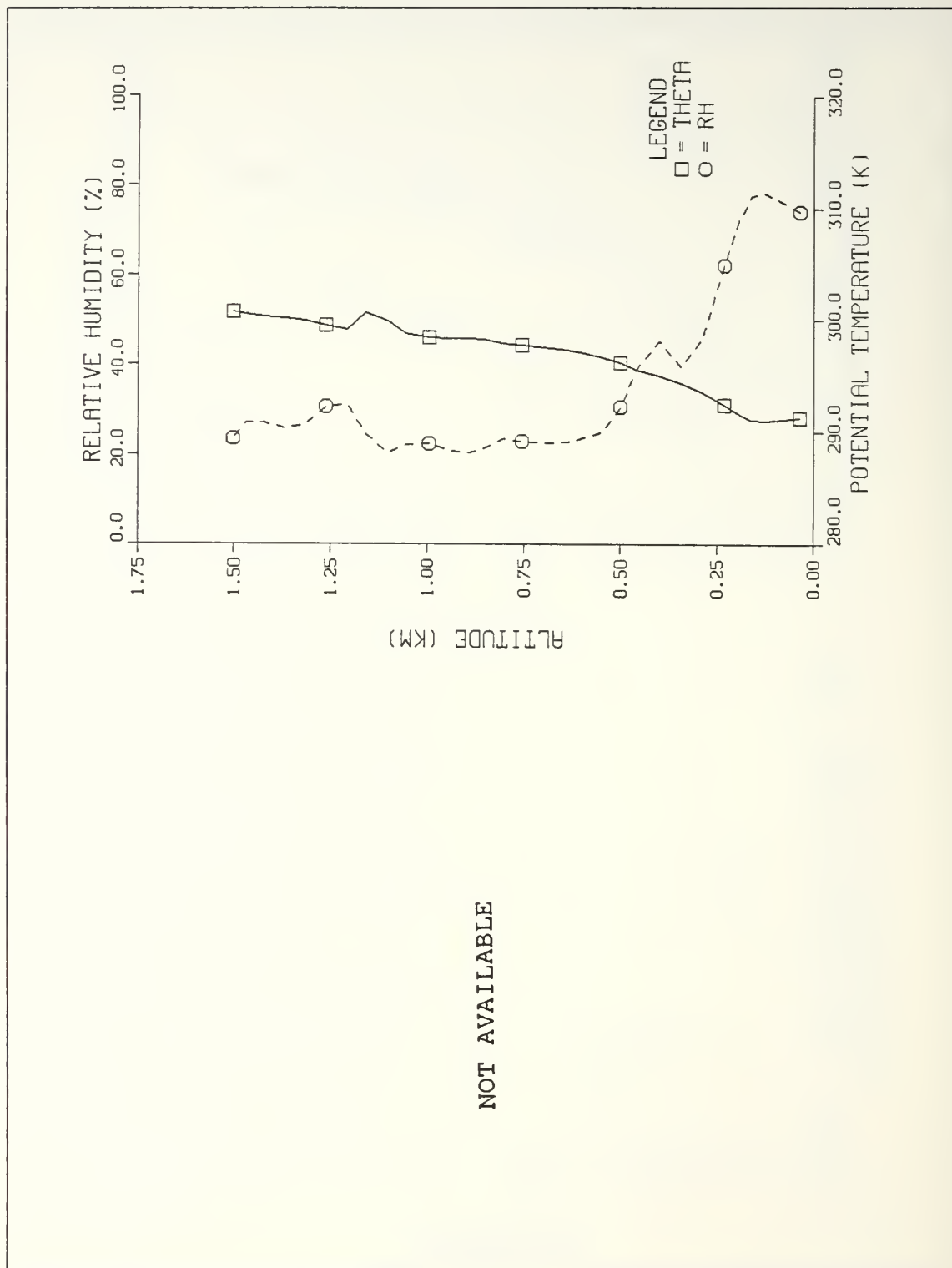
Figure A.16   Same as Fig. A.2 but for B on 1 Oct 1982.
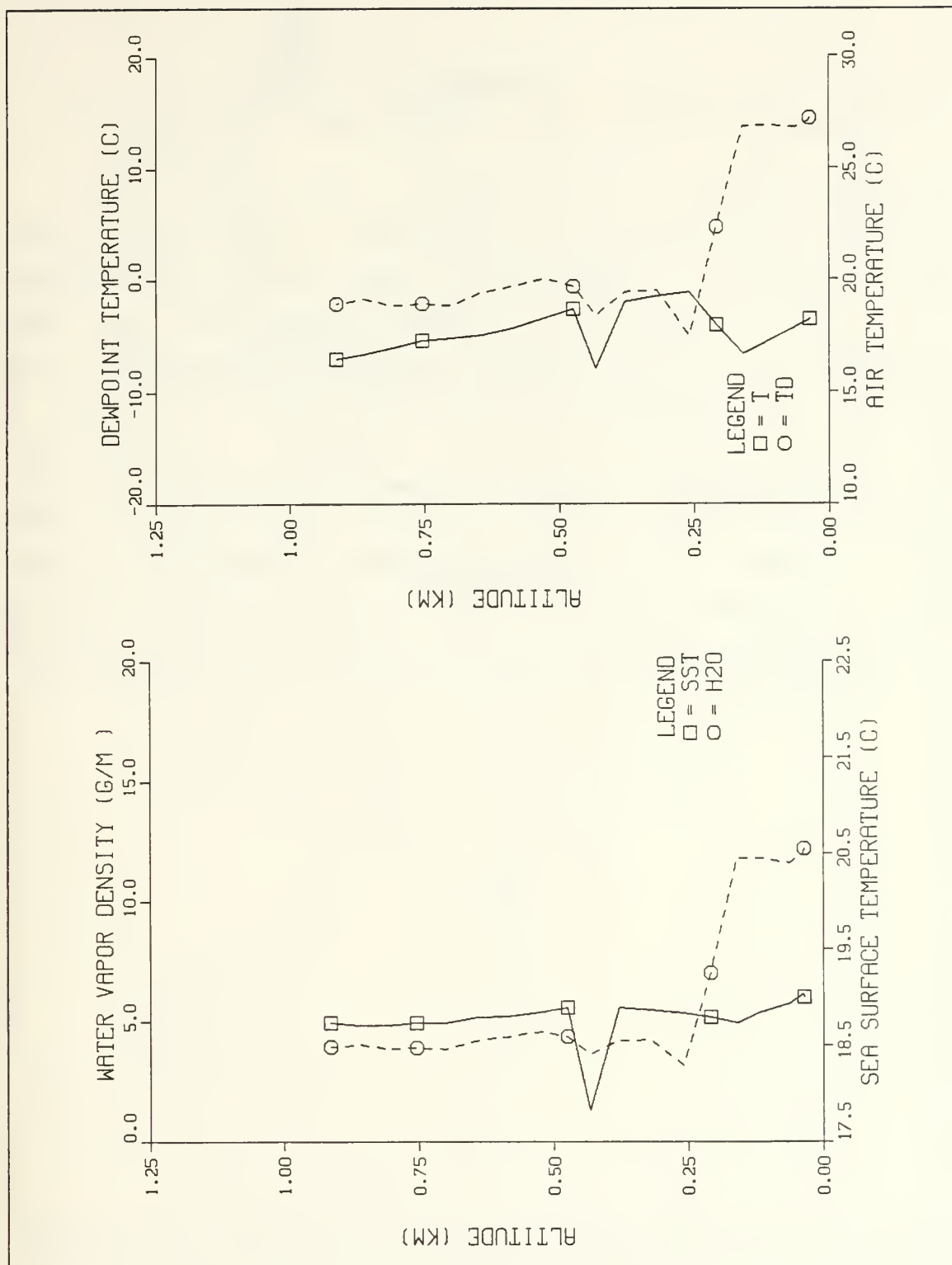
Figure A. 17   Same as Fig. A. 1 but for B1 on 1 Oct 1982.
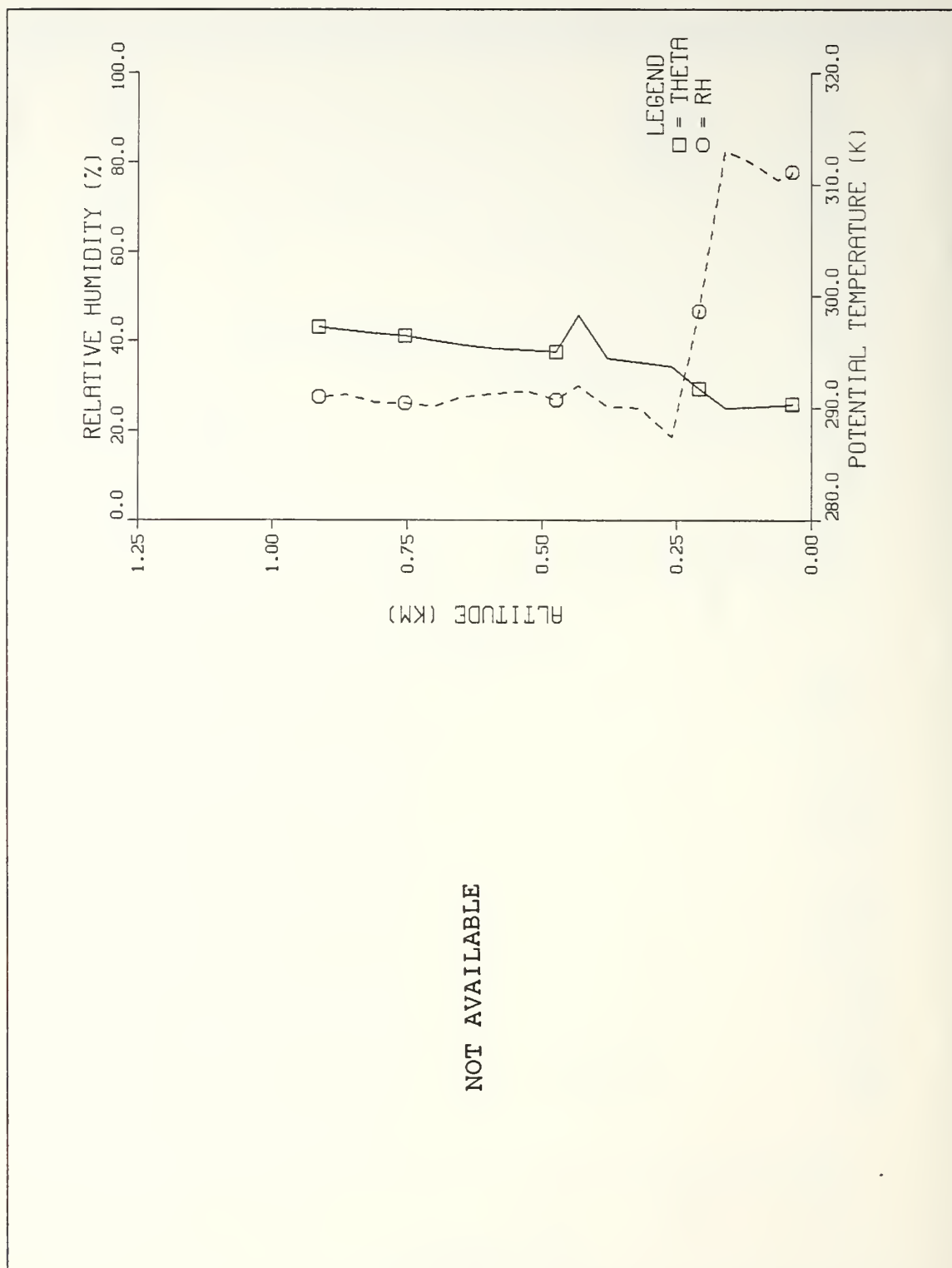
Figure A.18   Same as Fig. A.2 but for B1 on 1 Oct 1982.

AIRCRAFT PRT-5 AND LOWTRAN 6 SEA SURFACE TEMPERATURES

The figures show a comparison of aircraft radiometer (PRT-5) sea surface temperature measurements and LOWTRAN 6 computed sea surface temperatures (SST). The PRT-5 measured SST using wavelengths between 8 and 14 μm. Graph (a) in each figure shows LOWTRAN 6 computed SST for wavelengths of 8 and 11 μm without any aerosol contribution and the PRT-5 measured SST. Graph (b) shows the LOWTRAN 6 SST at 8 μm with and without the models aerosol distribution and the PRT-5 measured SST. The SST profiles that were computed using the LOWTRAN 6 "Navy Maritime" aerosol model are iden-tified with an "A" after the wavelength, such as 8A or 11A. Graph (c) in each figure shows the LOWTRAN 6 SST profile at 11 μm with (11A) and without (11) aerosol contributions.
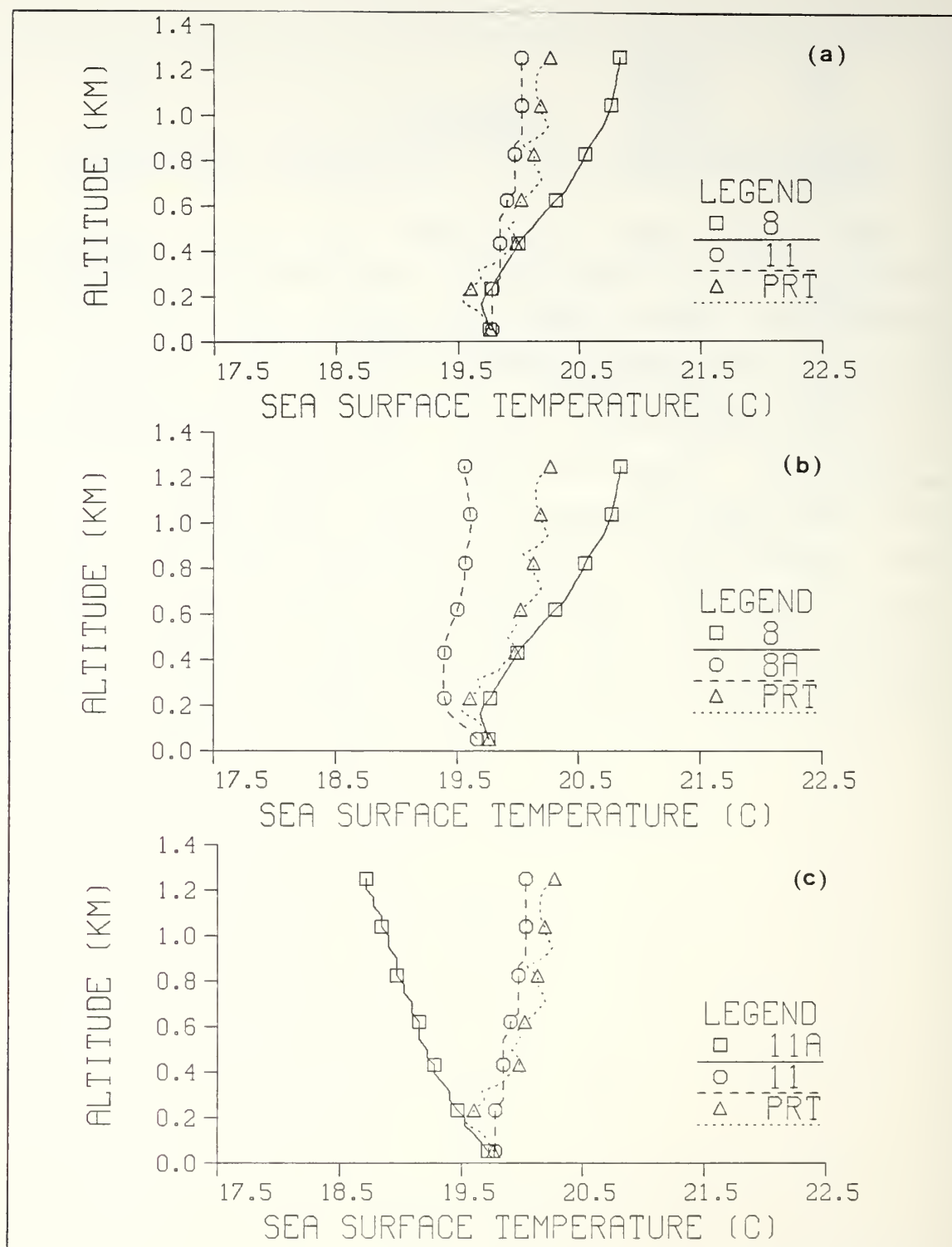
Figure B.1   Comparison of PRT-5 radiometer and
LOWTRAN 6 SST profiles with (8A) and without aerosols
for point B on 21 September 1982.

Figure B. 2   Same as Fig. B. 1 but for AB on 21 Sept 1982.
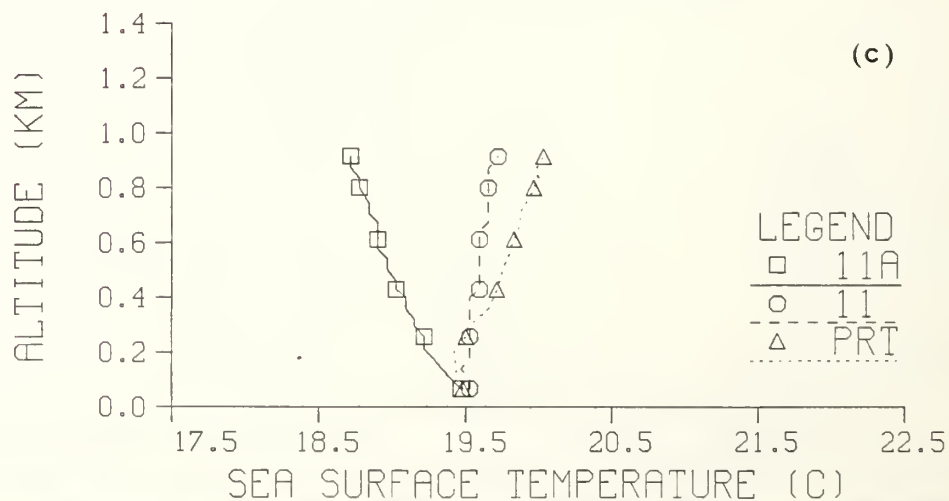
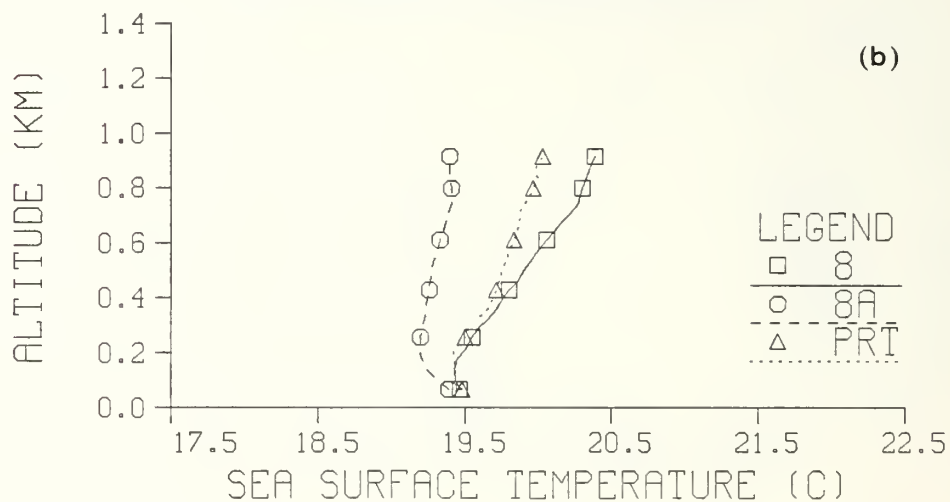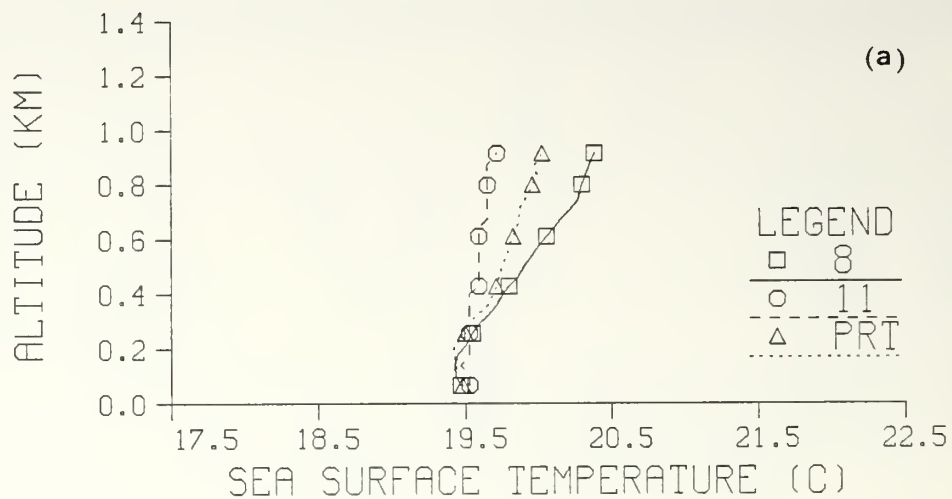Figure B.3   Same as Fig. B.1 but for A1 on 21 Sept 1982.
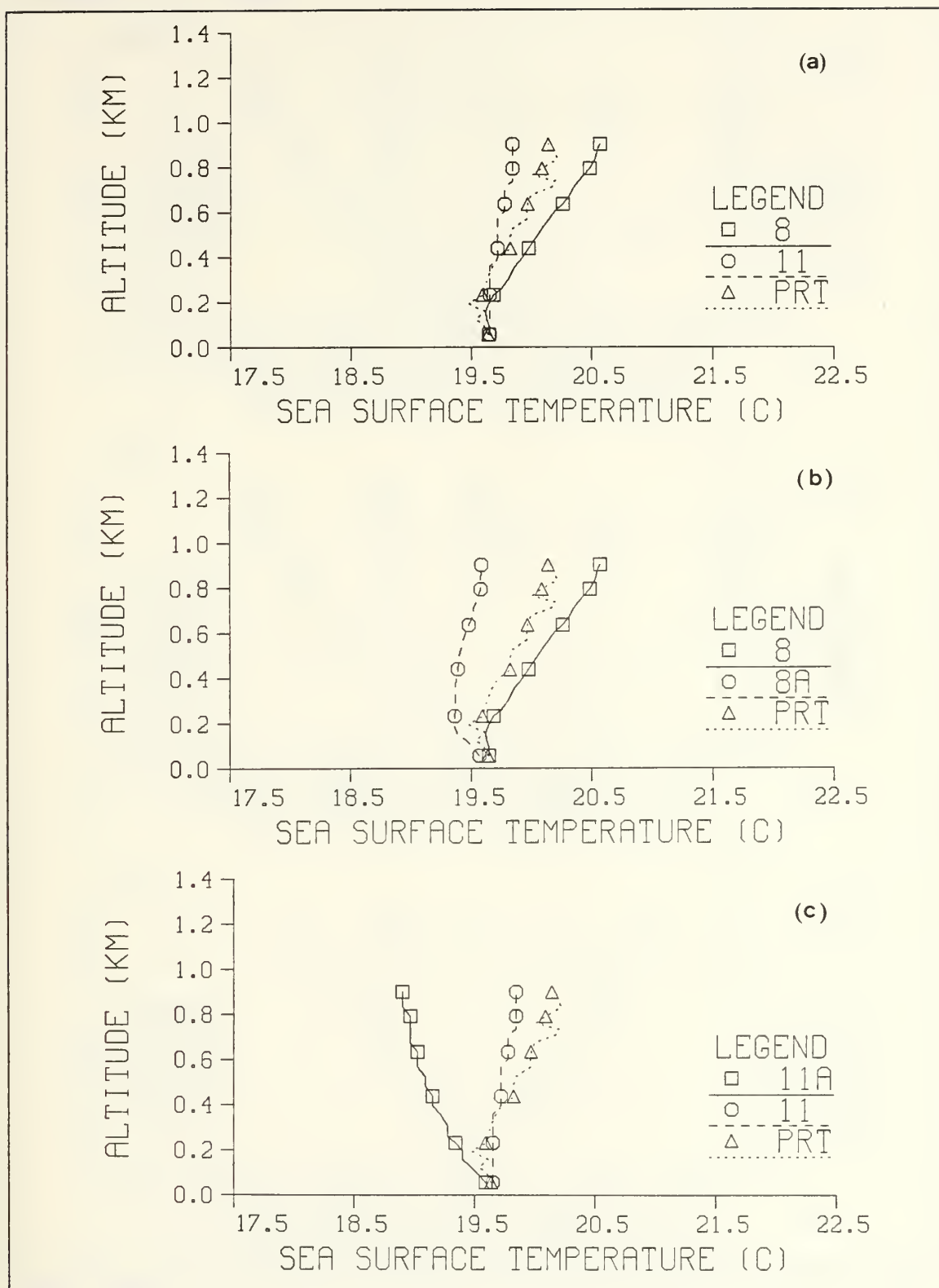
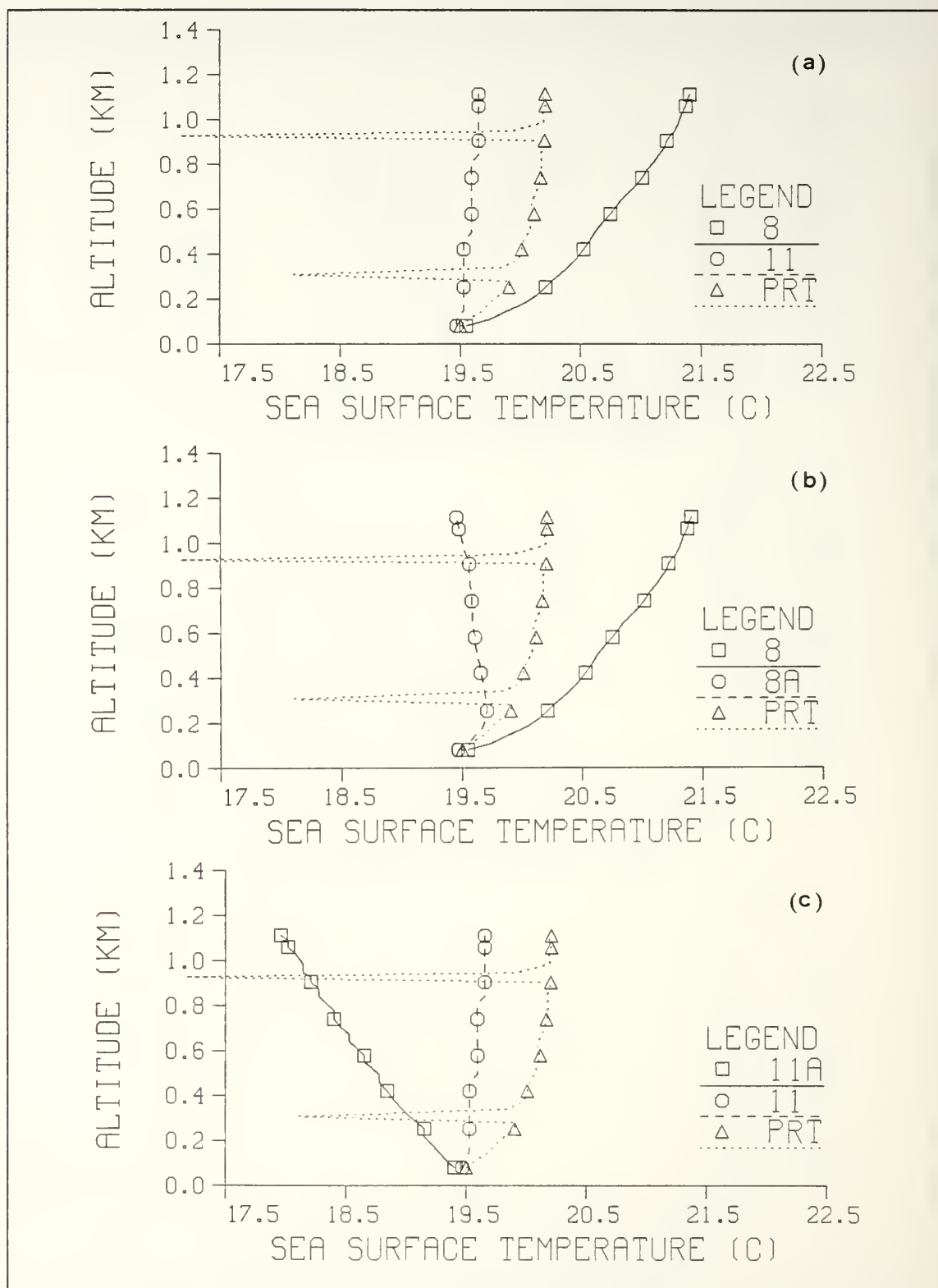Figure B.4   Same as Fig. B.1 but for B1 on 21 Sept 1982.

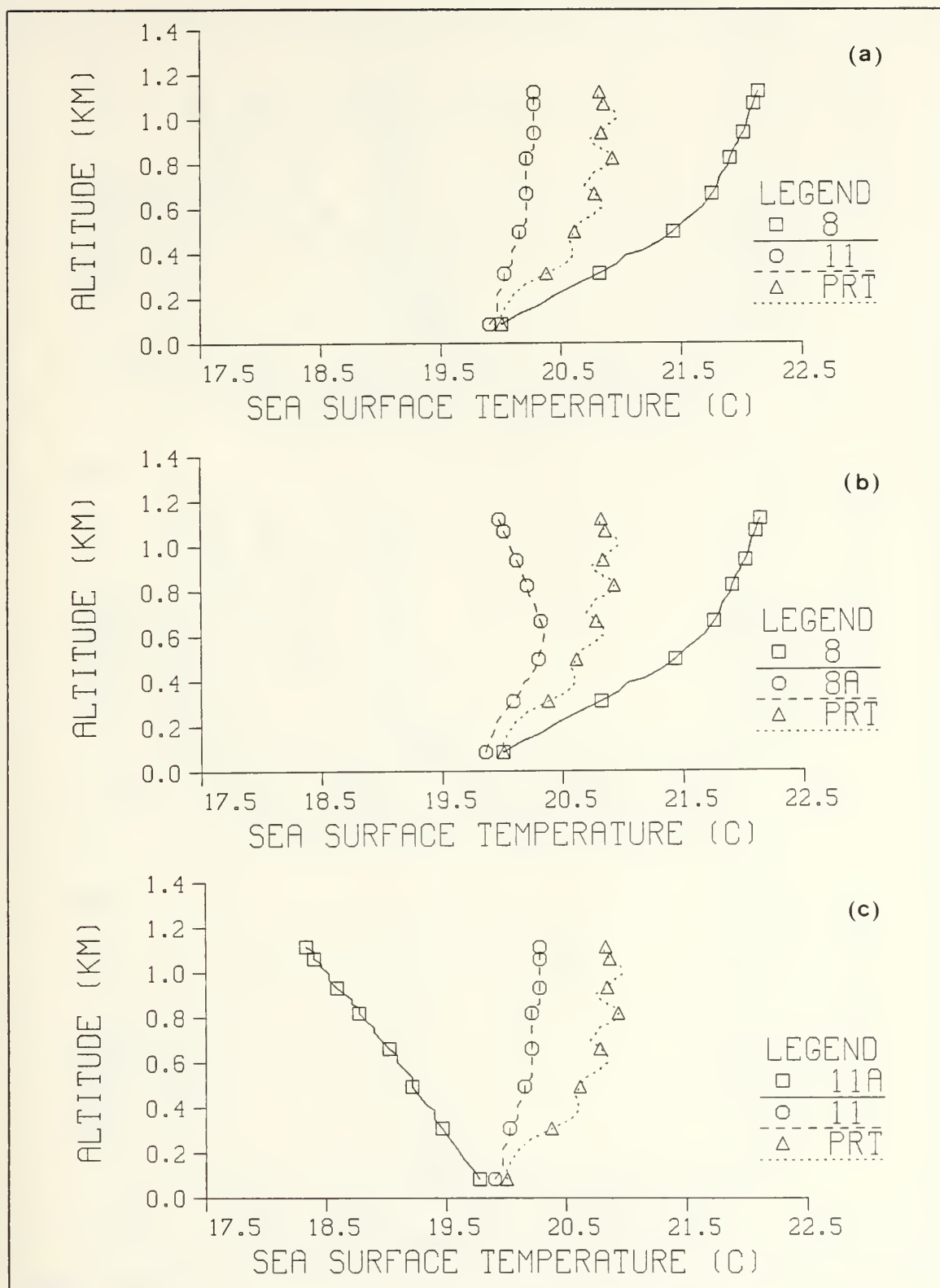Figure B.5   Same as Fig. B.1 but for B on 22 Sept 1982.

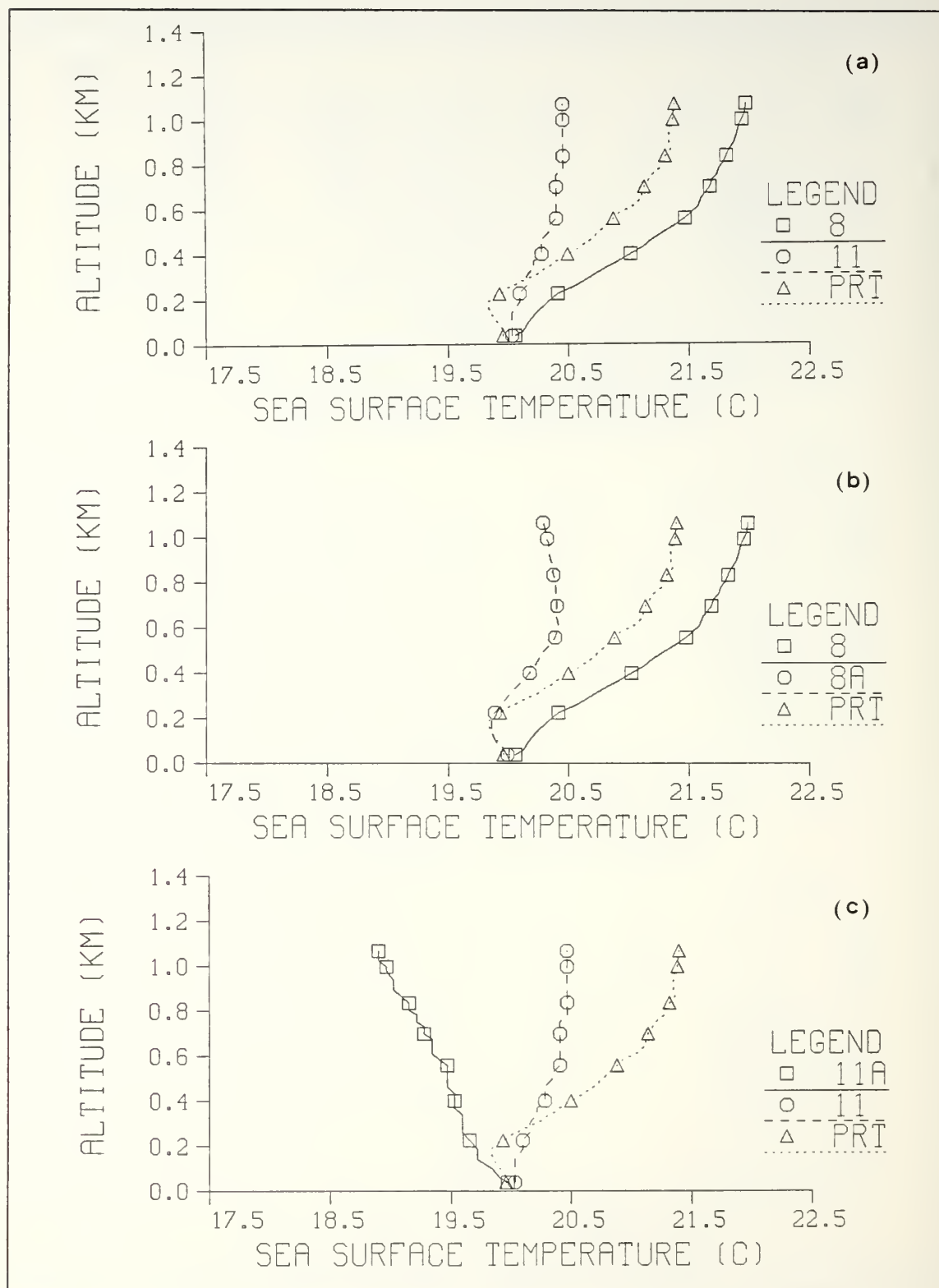Figure B.6   Same as Fig. B.1 but for B1 on 22 Sept 1982.

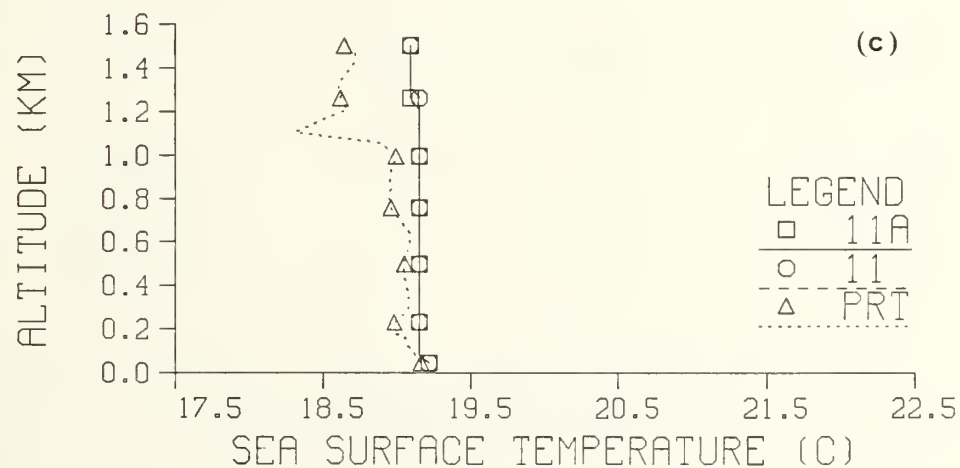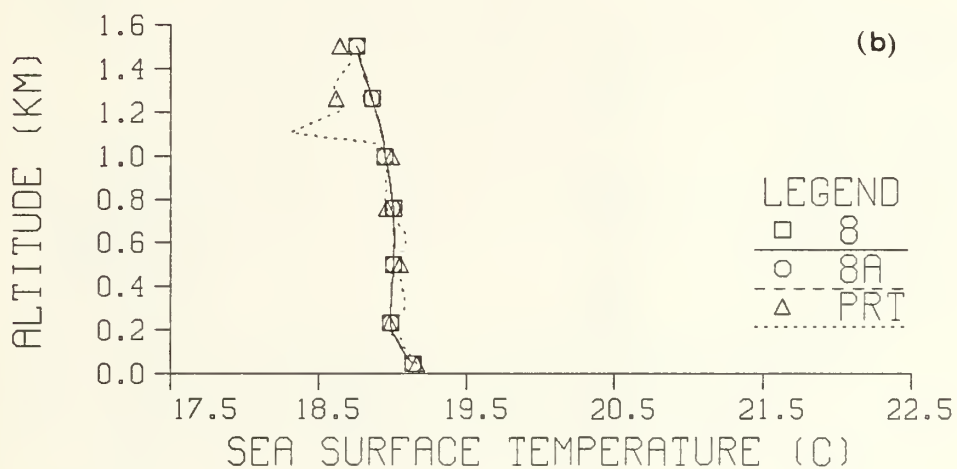Figure B. 7   Same as Fig. B. 1 but for A1 on 22 Sept 1982.
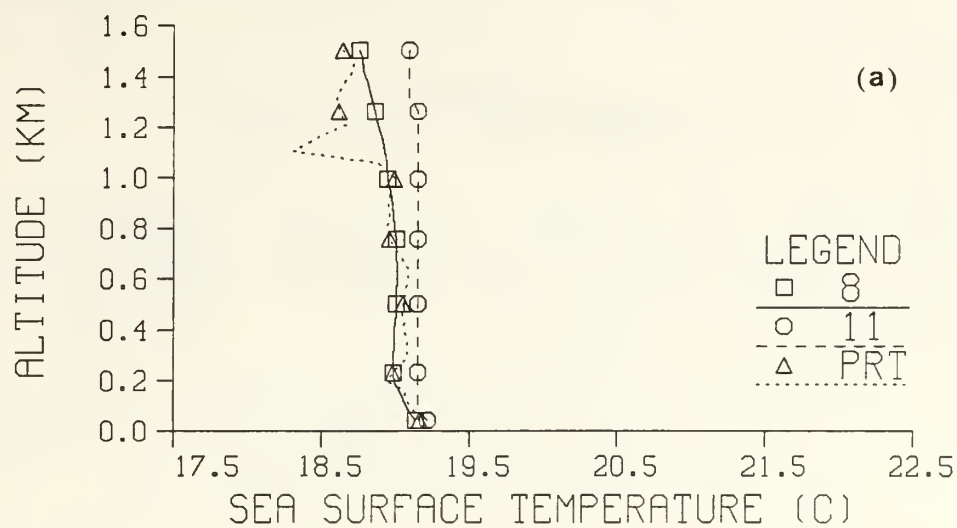
Figure B. 8   Same as Fig. B. 1 but for B on 1 Oct 1982.

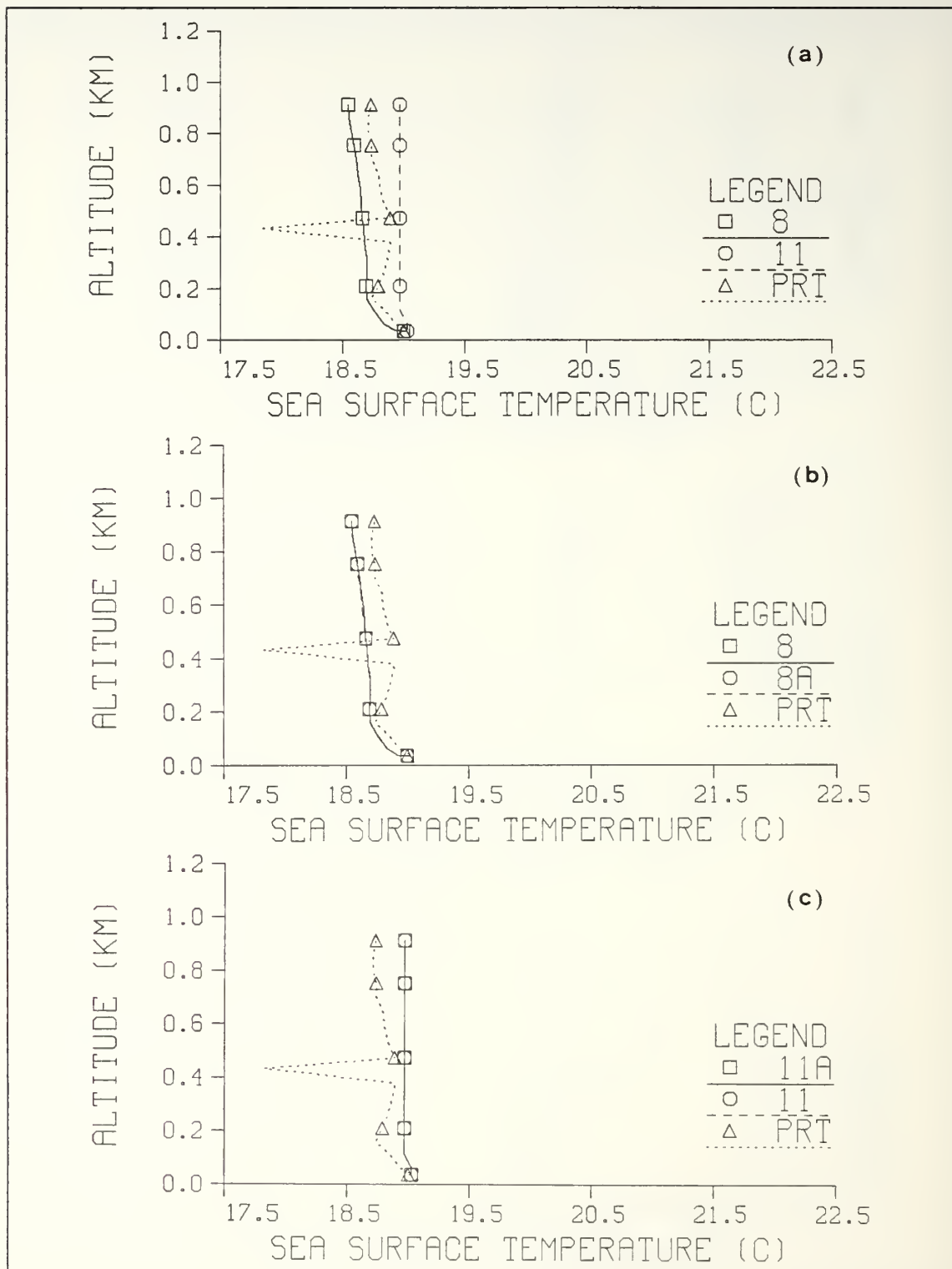Figure B.9   Same as Fig. B.1 but for B1 on 1 Oct 1982.

APPENDIX C
SAN NICOLAS ISLAND SOUNDINGS

This appendix contains the San Nicolas Island soundings taken in 21 and 22 September and 1 October 1982.
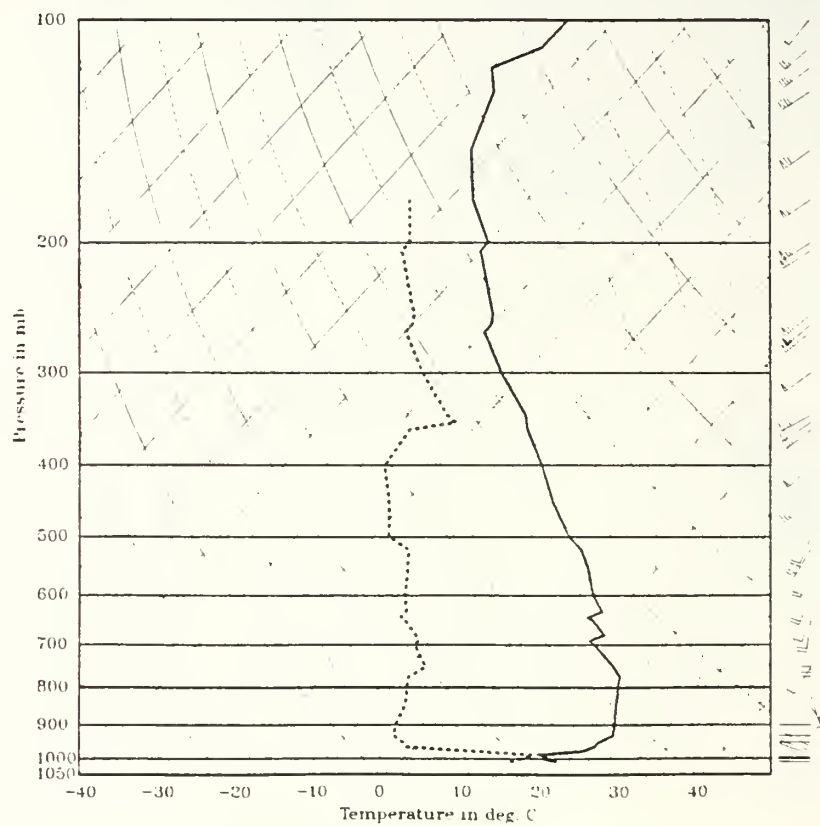
Figure C.1   San Nicolas Island sounding with
air and dewpoint temperature plots
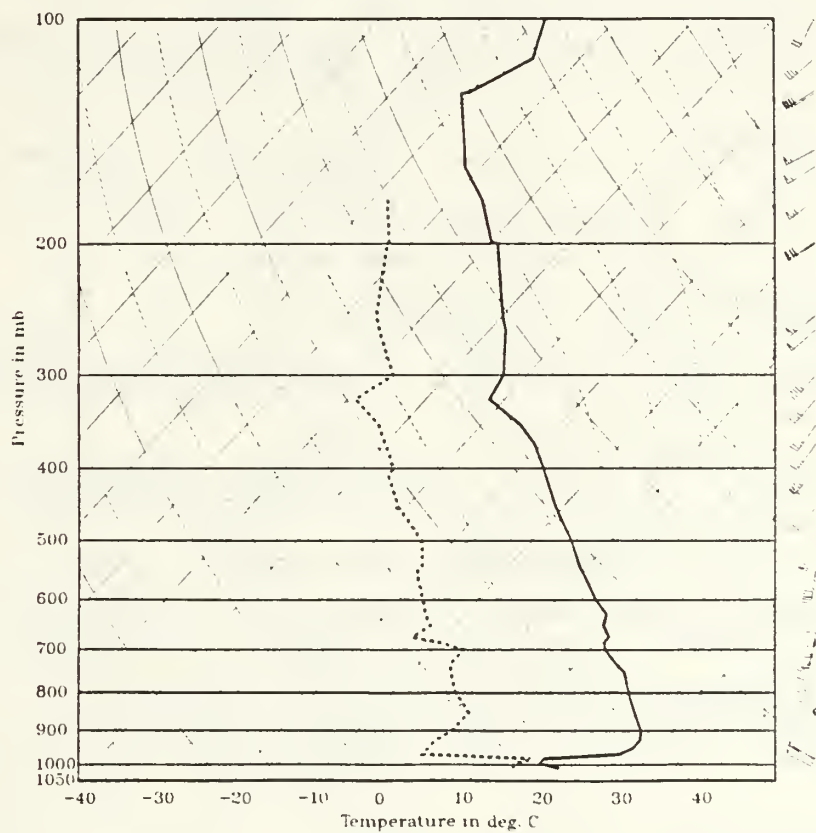and winds collected on 21 September 1982.

70

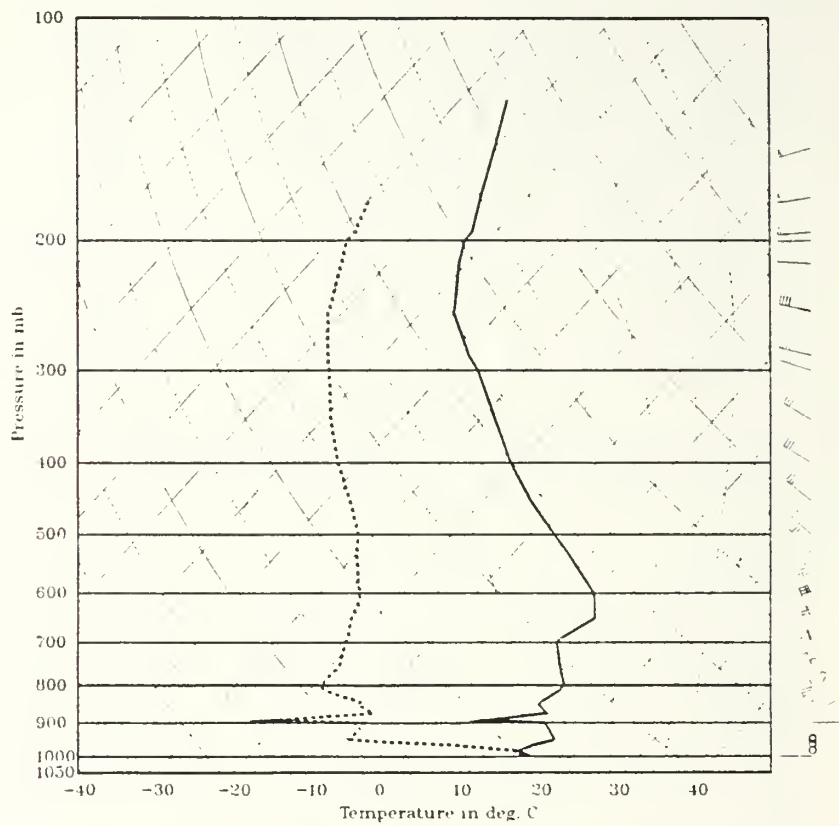Figure C. 2   Same as Fig. C. 1 but for 22 September 1982.

71

Figure C.3   Same as Fig. C.1 but for 1 October 1982.

LIST OF REFERENCES

Bolton, D., 1980: The Computation of Equivalent Potential Temperature. *Mon. Wea. Rev.*, *108*, 1046-1053

Durkee, P. A., E. E. Hindman, and T. H. Vonder Haar, 1984: The Detection of Marine Haze with Meteorological Satellites. In *Hygroscopic Aerosols in the Planetary Boundary Layer*, edited by L. H. Ruhnke and A. Deepak, A. Deepak Publishing, Hampton, VA., 171-180.

Durkee, P. A., 1984: *The Relationship Between Marine Aerosol Particles and Satellite- Detected Radiance*, Ph.D. Thesis, Colorado State University, Fort Collins, Colorado, US ISSN 0067-0340.

Fett, R. W., and R. G. Isaacs, 1979: Concerning Cause of 'Anomalous Gray Shades' in DMSP Visible Imagery. *J. Appl. Meteor.*, *18*, 1340.

Griggs M., 1983: Satellite Measurements of Tropospheric Aerosols. *Adv. Space Res.*, *2(5)*, 109-118.

Kneizys., F. X., E. P. Shettle, W. O. Gallery, J. H. Chetwynd, Jr., L. W. Abreu, J. E. A. Selby, S. A. Clough, and R. W. Fenn, 1983: *Atmospheric Transmittance/Radiance*: *Computer Code LOWTRAN 6*, AFGL-TR-83-0187.

Lauritson, L., G. J. Nelson, and F. W. Porton, 1979: Data Extraction and Calibration of TIROS-N/NOAA Radiometers. NOAA Tech Mem. Ness-107.

Liou, K. N., 1980: *An Introduction to Atmospheric Radiation*. Academic Press, New York.

McAlister, E. D., and W. McLeish, 1969: Heat Transfer in the Top Millimeter of the Ocean. *J. Geophys. Res.*, *74*, 3408-3414.

McClain, E. P., 1980: Multiple Atmospheric-Window Techniques for Satellite-Derived Sea Surface Temperatures. *Oceanography from Space*. edited by J. F. R. Gower. Plenum Press. New York, N.Y. 73-85.

McClain, E. P., W. G. Pichel, C. C. Walton, Z. Ahmad, and J. Sutton, 1983: Multi-channel Improvements to Satellite-Derived Global Sea Surface Temperatures *Adv. Space Res.* *2(6)*, 43-47.

Kidwell, K. B., 1984: *NOAA Polar Orbiter Data Users Guide*, NOAA National Environmental Satellite, Data, and Information Service, World Weather Building, Washington, D.C.

Noonkester, V. R., 1980: Marine Aerosols and Calculated Optical Properties in a Convective Layer Near San Nicolas Island. Technical Note 925, Naval Ocean Systems Center, San Diego, CA.

Noonkester, V. R., 1981: Aerosol Size Spectra in a Convective Marine Layer with Stratus: Results from Airborne Measurements near San Nicholas Island, Ca. *J. Appl. Meteor.*, *20*, 1076-1080.

Strong, A. E., and E. P. McClain, 1984: Improved Ocean Surface Temperatures from Space-Comparisons with Drifting Buoys. _Bull_. _Amer_. _Meteorol_. _Soc_., _65_, 138-142.

Tetens, O., 1930: Uber einige meteorologische Begriffe. _Z_. _Geophys_., _6_, 297-309.

INITIAL DISTRIBUTION LIST

		No. Copies
1.	Defense Technical Information Center Cameron Station Alexandria, VA 22314-6145	2
2.	Library, Code 0142 Naval Postgraduate School Monterey, CA 93943-5000	2
3.	Chairman, Code 68 Department of Oceanography Naval Postgraduate School Monterey, CA 93943	1
4.	Chairman, Code 63 Department of Meteorology Naval Postgraduate School Monterey, CA 93943	1
5.	Professor Philip A. Durkee, Code 63De Department of Meteorology Naval Postgraduate School Monterey, CA 93943	5
6.	Professor Roland Garwood, Code 63Gd Department of Oceanography Naval Postgraduate School Monterey, CA 93943	2
7.	Director Naval Oceanography Division Naval Observatory 34th and Massachusetts Avenue NW Washington, DC 20390	1
8.	Commander Naval Oceanography Command NSTL Station Bay St. Louis, MS 39522	1
9.	Commanding Officer Naval Oceanographic Office NSTL Station Bay St. Louis, MS 39522	1
10.	Commanding Officer Fleet Numerical Oceanography Center Monterey, CA 93940	1
11.	Commanding Officer Naval Ocean Research and Development Activity NSTL Station Bay St. Louis, MS 39522	1
12.	Commanding Officer Naval Environmental Prediction Research Facility Monterey, CA 93940	1
13.	Chairman, Oceanography Department U.S. Naval Academy Annapolis, MD 21402	1

14. Chief of Naval Research   1
     Naval Ocean Research and Development Activity
     800 N. Quincy Street
     Arlington, VA 22217

15. Office of Naval Research, Code 420   1
     Naval Ocean Research and Development Activity
     800 N. Quincy Street
     Arlington, VA 22217

16. Scientific Liason Office   1
     Office of Naval Research
     Scripps Institution of Oceanography
     La Jolla, CA 92037

17. Library   1
     Scripps Institution of Oceanography
     P.O. Box 2367
     La Jolla, CA 92037

18. Commander   1
     Oceanographic Systems Pacific
     Box 1390
     Pearl Harbor, HI 96860

19. Library Aquisitions   1
     National Center for Atmospheric Research
     P.O. Box 3000
     Boulder, CO 80307

20. LT. S.K. Runco   2
     6625 Mill St.
     Sylvania, OH. 43560